5-2018

Lead Doped Carbon Nanofibers in Li-ion Batteries

Omar Torres
The University of Texas Rio Grande Valley

LEAD DOPED CARBON NANOFIBERS

IN LI-ION BATTERIES

A Thesis

by

OMAR TORRES

Submitted to the Graduate College of
The University of Texas Rio Grande Valley
In partial fulfillment of the requirements for the degree of

MASTER OF SCIENCE ENGINEERING

May 2018

Major Subject: Mechanical Engineering

LEAD-DOPED CARBON NANOFIBERS

IN LI-ION BATTERIES

A Thesis
by
OMAR TORRES

COMMITTEE MEMBERS

Dr. Karen Lozano
Chair of Committee

Dr. Mataz Alcoutlabi
Committee Member

Dr. Javier Ortega
Committee Member

May 2018

ABSTRACT

Torres, Omar, Lead-doped Carbon Nanofibers in Li-Ion Batteries, Master of Science Engineering (MSE), May, 2018, 70 pp., 2 tables, 44 figures, references, 74 titles.

Lead acid batteries have been a very reliable rechargeable battery since its inception in the mid-1800s. Lithium-Ion batteries have been sought out for their light-weight and capacity of holding large amounts of energy in a small amount of space. Few studies have been conducted in the use of lead in lithium-ion batteries.

In this thesis, lead-doped carbon nanofibers were produced by using the Forcespinning® method and used as an anode on a lithium-ion battery. The morphology, material characterization and thermal properties of the anode material were analyzed using the Scanning Electron Microscopy (SEM), Energy Dispersive X-Ray Spectroscopy (EDS), Thermogravimetric Analysis (TGA) and X-Ray Photoelectron Spectroscopy (XPS). Electrochemical studies on the batteries cells were cycle performance, cyclic voltammetry and rate performance.

DEDICATION

I dedicate this work to God, who has always been there with me every step of the way. To my father, whose wise words kept me on track to graduate. To my mother, whose warm attitude gave me optimism. To my brothers, who show that it is never too late to go back and rebuild. And finally, to Charlotte whose love and unconditional support was always there when I needed it.

ACKNOWLEDGMENTS

I would like to thank my Committee Chair and adviser Dr. Karen Lozano for all of her guidance, support and patience since I first came into her office as a freshman 10 years ago. She has always welcomed me, first as an undergraduate, later as a professional and until recently, as a graduate student. To my committee members, Dr. Mataz Alcoutlabi and Dr. Javier Ortega, who over the past two years have become more than my professors, but also as great friends.

To all my loved ones, co-workers and students I've encountered during my time in UTRGV and across the United States while meeting in conferences. Thank you for the support and you will always have my gratitude.

This project is supported by NSF PREM award under grant No. DMR-1523577: UTRGV-UMN Partnership for Fostering Innovation by Bridging Excellence in Research and Student Success.

TABLE OF CONTENTS

Page

ABSTRACT……...……iii

DEDICATION……iv

ACKNOWLEDGEMENTS…….v

TABLE OF CONTENTS……vi

LIST OF TABLES…….……..viii

LIST OF FIGURES……...…….ix

CHAPTER I. INTRODUCTION…….……1

CHAPTER II. REVIEW OF LITERATURE……..…3

2.1 Introduction……..…3

2.2 Lead-Acid Batteries (LABs)……3

2.3 Types of Lead-Acid Batteries……..6

2.4 LAB Problems and Drawbacks……9

2.5 Lithium-Ion Batteries (LIBs)…….……11

2.6 Types of Lithium-Ion Batteries……..……13

2.7 LIB Problems and Drawbacks……..……15

2.8 Carbon……17

2.9 Nanotechnology…….……19

CHAPTER III. EXPERIMENTAL SETUP ……...……..23

3.1 Introduction…….…….. 23

3.2 Fabrication Equipment…….……..23

3.3 Characterization Analysis……..24

3.4 Electrochemical Analysis……...……30

CHAPTER IV. EXPERIMENTAL PROCEDURE ……..……32

4.1 Materials Used……...……32
4.2 Solution Process…….……32
4.3 Fiber Production…….……34
4.4 Carbonization Process……..……..35
4.5 LIB Assembly……36
CHAPTER V. RESULTS & DISCUSSION ……...…….39
5.1 Characterization…….39
5.2 Electrochemical Analysis……..…….45
5.3 Post-Mortem Analysis……...……51
5.4 Discussion……..……56
CHAPTER VI. CONCLUSION & FUTURE WORK……..……58
6.1 Conclusion…….……58
6.2 Future Work……...……59
REFERENCES……..……60
APPENDIX A……66
BIOGRAPHICAL SKETCH…….……70

LIST OF TABLES

Page

Table 1: List of solutions used to spin into fibers ……..…32

Table 2: Visual quantity of fibers produced when spinning 1 mL of solution……..33

LIST OF FIGURES

Page

Figure 1: Schematic representing a flooded LAB……4

Figure 2: LAB chemical equation……6

Figure 3: Diagram of the specific energy density and volumetric energy density of the most common batteries in the industry……12

Figure 4: Schematic of a lithium ion cell……...13

Figure 5: Types of LAB configurations with carbon……17

Figure 6: Schematic drawing of a typical setup inside the Cyclone showing the spinneret, collectors, fan assembly……24

Figure 7: Schematic representation of an SEM……25

Figure 8: Zeiss SEM used to characterize the fibers……..26

Figure 9: Schematic representation of the EDS spectra……27

Figure 10: Constant heating rate equation……28

Figure 11: TA Model 400 used to analyze fibers……..28

Figure 12: The XPS was used to measure the elemental composition of the fibers……..29

Figure 13: Battery load station to the Autolab 128N……30

Figure 14: A sample prepared in scintillation vials and sealed with parafilm prior heated oil bath……..33

Figure 15: Cyclone L1000 used to produce the PVA-Pb fibers……34

Figure 16: Dehydration of mat prior carbonization……...35

Figure 17: GSL – 1700X used to carbonize PVA-Pb fiber mats……...36

Figure 18: Two Lead Carbon Anodes punches from carbonized mat……..…..37

Figure 19: Half-cell lithium-ion battery assembly ……37

Figure 20: SEM image from a lead carbon sample at 750X……..39

Figure 21: SEM image from a lead carbon sample at 10KX……..…40

Figure 22: SEM image from a lead carbon sample at 25KX…….40

Figure 23: Section of the fiber analyzed with the EDS to determine the material characterization……41

Figure 24: Section of the fiber analyzed with the EDS to determine material characterization…41

Figure 25: EDS Spectra of the lead carbon sample in Figure 23……...42

Figure 26: EDS Spectra of the lead carbon sample……...42

Figure 27: EDS mapping of the lead carbon fibers showing a 44% Pb content distributed evenly among the fibers…….43

Figure 28: TGA analysis of PVA, PVA-Pb & Lead Carbon fibers……..43

Figure 29: XPS spectra showing spectra of C1s, O1s & various Pb in the fiber……...44

Figure 30: XPS spectra of the Pb4f scan……...45

Figure 31: Columbic Efficiency of the carbon fiber anode performed after 100 cycles at a current density of 100 mAg^{-1}…….46

Figure 32: Cycle Performance of the carbon fiber anode performed after 100 cycles at a current density of 100 mAg^{-1}…….46

Figure 33: Columbic Efficiency of the lead carbon fiber anode performed after 100 cycles at a current density of 100 mAg^{-1}…….47

Figure 34: Cycle Performance of the lead carbon fiber anode performed after 100 cycles at a current density of 100 mAg^{-1}……..48

Figure 35: Cyclic Voltammetry of carbon fibers between 0.01 and 3.0 V at a scan rate of 0.1 mVs^{-1}……..49

Figure 36: Cyclic Voltammetry of lead carbon fibers between 0.01 and 3.0 V at a scan rate of 0.1 mVs^{-1}……50

Figure 37: Rate performance for the lead carbon anode performed at current densities of 50, 100, 200, 400 and 500 mAg^{-1}…….51

Figure 38: SEM imaging of the post cycled lead carbon anode at 1KX……52

Figure 39: SEM imaging of the post cycled lead carbon anode at 10KX……..53

Figure 40: SEM imaging of the post cycled lead carbon anode at 25KX……..53

Figure 41: SEM imaging of the post cycled lead carbon anode at 25KX……..54

Figure 42: EDS image for the post cycled lead carbon anode……...55

Figure 43: Elemental analysis mapping for the post cycled lead carbon anode……....55

Figure 44: Comparison from the specific capacities from the study mentioned earlier compared to results gathered in the lab with the lead carbon anode……..….56

CHAPTER I

INTRODUCTION

Since the origin of the lead-acid battery, many rechargeable batteries have been developed, the lithium-ion battery is the most popular to date.[1] Both lead-acid and lithium-ion batteries are almost complete opposites when it comes to their capabilities however in principle they function similar.[2]

For the past couple of years there has been an interest in the battery industry and the scientific community in exploring the possibility combining lead and lithium to potentially improve the performance and capabilities of both batteries. There have been few studies have been conducted in the lab due to the toxicity of lead and hazard is present to the environment when not disposed or recycled properly. Due to these concerns the battery industry in general is gearing toward using less lead because of this.[3]

However, the consumption of lithium globally has been increasing at an exponential rate and if the rate of consumption does not stabilize or decrease, we could see ourselves running out of lithium in a few decades.

Lead can still provide further use and has not been as investigated as its counterpart. With the use of nanotechnology, its high recyclability and its affordability; lead can potentially give the industry a cheaper, safer and affordable option by exploring the material further.

There are two parts to accomplish in this thesis, first, the development and optimization of lead-doped carbon nanofibers through centrifugal spinning, technology developed at The

University of Texas Pan-American by Dr. Karen Lozano that resulted in the first startup at the university, a company named Fiberio Technology Corporation. The second part of this thesis is to use the newly developed material anodes in half-cell Li-ion batteries and characterize its electrochemical performance.

Chapter 2 focuses on providing a literature review to lead-acid and lithium-ion batteries and the effect that nanotechnology has had on battery development over the last couple of decades. This chapter introduces the reader to different types of batteries, mostly related to lead and lithium batteries as well as depicting processes used to manufacture these batteries with their respective characterization.

Chapter 3 presents the instrumentation used throughout the project. The theory, principles and specific functions are described.

Chapter 4 presents the experimental setup and procedures used to develop the fibers as well as its characterization and electrochemical testing parameters.

Chapter 5 presents the results and discussion related to the characterization and electrochemical tests conducted on the lead-doped carbon nanofibers and lead-lithium-ion batteries.

Chapter 6 concludes with lessons learned and presents an overview of future work that could help improve the production of lead-doped carbon nanofibers and lead-lithium-ion batteries.

CHAPTER II

REVIEW OF LITERATURE

2.1 Introduction

The origin of this research began with advances made in the production of carbon fibers used as anodes for Li-ion batteries and the need to further improve the electrochemical performance of these batteries. There is a strong push to move away from lead, through there are many advantages that could play a pivotal role in the manufacturing of affordable and reliable lead batteries though with significantly less lead content given the use of lead-based nanofiber membranes; and thus, worth exploring. Throughout the literature review it was found that lead has been tested in Li-ion batteries.

The literature review will be divided into 3 sections: Lead-acid batteries, Lithium-Ion batteries and Carbon.

2.2 Lead-Acid Batteries (LABs)

Lead-acid batteries (LABs) have come a long way from its initial inception when Gaston Plante initially introduced the word, his discovery dates back to 1859.[4] The structure of the LAB has not changed much since still consists of; plates, separators and an electrolyte. Figure 1 represents a basic schematic of a LAB.

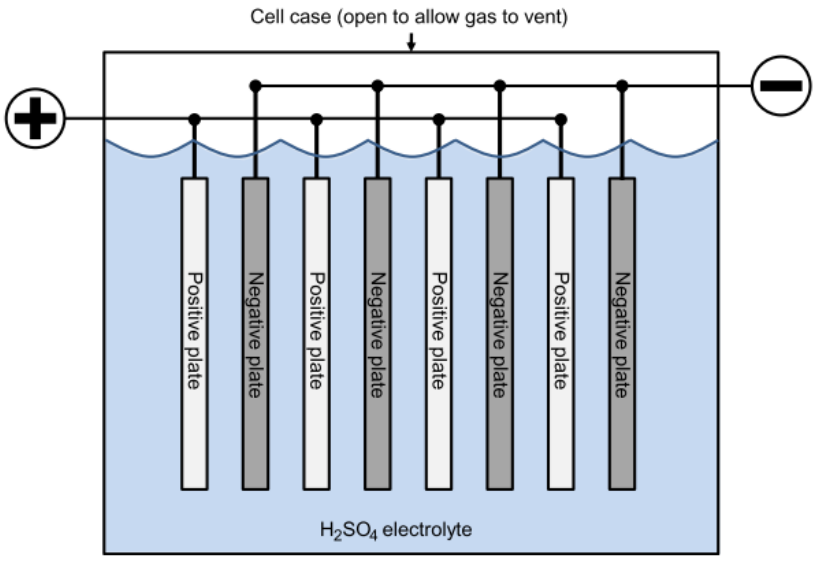

Figure 1 – Schematic representing a flooded LAB.[5]

2.2.1 Plates

Plates is a synonym for batteries electrodes. These are placed in series to add up to the voltage needed to be produced. The most common type of plates is composed of Lead and Lead Oxide (also referred to leady oxide). When submerged in a diluted solution of sulfuric acid, a circuit is made and the battery starts to discharge. These plates are made up of a metallic grid and the active material that is placed on the grid and later submerged in the electrolyte. The first grids used were of pure lead, this later proved to be troublesome since the material is too soft and cannot support itself. Manufacturers began adding different type of materials into the grid to increase its mechanical strength and improve electrical properties.

A study conducted by Alex Nuzhny explored into the effects of corrosion of low-antimony lead-cadmium alloys in continuous operation in a LAB.[6] It was found that low-antimony lead-cadmium alloy doped by silver and selenium possessed significant resistance compared to pure lead grids. It was also found that the increased corrosion resistance of the alloy

was done specifically through the reduction of grains and the suppression of development of highly branched dendrites.

A common problem for plates it's the aggregation of lead sulfate particles in the electrode may result in a reduced capacity plate. Another modification that can be done to the plates is to modify the surfaces of the grids. A study conducted by M.S. Rahmanifar, lead grids were anodized to produce a layer of lead dioxide that interacts with aniline solution and produces polyanile which reduced the accumulation of lead sulfate in the grids.[7]

Investigations have also looked into reducing the weight of the battery through using lighter materials. Such studies are like the one conducted by Liang-xing Jiang *et al*, where the Pb plated Al was investigated.[8] It was found that not only the weight of the Al/Pb was 55.4% lighter than the Pb-alloy grid, but it also reduced the electrical resistance of the plate which improved its conductivity and had a lower internal resistance.

2.2.2 Separators

The separators are placed in between the opposite charging plates to insulate the plates to prevent short-circuiting each other but still maintain adequate permeability to allow the electrolyte to flow therefore promoting the free travel of electrons when the battery is either charging or discharging.

The initial LAB prototypes used a variety of materials for the separators, for example strips of rubber (first one tried by Gaston Plante) to wood, rubber glass fier mate, cellulose and other polymeric materials.

2.2.3 Electrolyte

The electrolyte of a battery is the chemical medium that is needed in order to allow the flow of ions between the cathode and anode. The electrolyte found in the lead acid battery is a diluted form of sulfuric acid (H_2SO_4). Different LABs will have different dilutions; however, they are close to 35-38% diluted with water when the LAB is fully charged. When the battery is discharged, the electrolyte is mainly composed of water. This is due for the chemical reaction that happens within the electrolyte and the electrodes in the battery.[9]

$$\text{anode: } \mathrm{Pb} + \mathrm{SO_4^{2-}} \rightarrow \mathrm{PbSO_4} + 2\mathrm{e^-}$$

$$\text{cathode: } \mathrm{PbO_2} + \mathrm{SO_4^{2-}} + 4\mathrm{H^+} + 2\mathrm{e^-} \rightarrow \mathrm{PbSO_4} + 2\mathrm{H_2O}$$

$$\text{net: } \mathrm{Pb} + 2\mathrm{H_2SO_4} + \mathrm{PbO_2} \rightarrow 2\mathrm{PbSO_4} + 2\mathrm{H_2O}$$

Figure 2 – LAB chemical equation.[10]

Figure 2 shows the electrochemical reaction that takes place within the LAB while its discharging. The anode of the LAB is Pb (also known as spongy lead) and the cathode is PbO_2, when the battery is being discharged, both electrodes become lead sulfate ($PbSO_4$, also known as sulfation). While the battery is being charged, the reaction that took place while it was discharging is reversable and reconverts the electrons back to their original elements.

2.3 Types of Lead-Acid Batteries

The most common LABs are starting, lighting & ignition batteries (SLI), stationary batteries and/or deep-cycle batteries. LABs can either be designed to focus on either power or energy density.[11] In cases where power delivery is needed, the more surface area where the

electrolyte is interacting with the electrodes the more power dense the battery will become for a short period of time. This is due to the sulfation process that the LAB goes through during the electrochemical process while discharging. When lead sulfate particles are formed in the surface of the electrode, there is less active material of which the electrolyte can react with.

In order to counter this, when an energy dense LAB is designed the following either need to happen: 1) increase the size of the electrode, 2) increase the distance between the electrode and 3) have a larger space at the bottom of the battery.

In order for the battery to be more energy dense, it will need more material for the electrolyte to interact with. In order to accomplish this the size of the electrode must increase. Due to the formation of $PbSO_4$, these crystals form at the surface of the electrodes which increase them in size which increase the probability of the battery of suffering a pre-mature failure by short-circuiting. In order to counter this from happening, the distance between the electrodes so when these crystals form on the electrode it does not touch the other electrode. For the last point, these $PbSO_4$ crystals are large enough that they fall from the surface of the electrode and accumulate at the bottom of the battery. This raises the possibility of having a large amount of $PbSO_4$ at the bottom that it can create a path from one electrode to another one which causes a short-circuit in the battery. To counter this, a larger space at the bottom of the battery so the $PbSO_4$ particulates can accumulate without risking touching either of the electrodes.

2.3.1 Starting, Lighting & Ignition batteries (SLI)

These are the most common LABs. An SLI battery is commonly used in automobiles as their starting battery that cracks the alternator to life. The job of this battery is to deliver a high current which discharges the battery, functions like a supercapacitor, once the alternator gets

going, the SLI battery recharges to its original level. These types of batteries are not designed to be for deep discharge.

In order to deliver large current, this battery has multiple thin parallel plates (approx. 0.50 mm) in order to increase the maximum surface area.[12] Although it could deliver a large current, it will damage the battery if it goes through a deep discharge. This is where it depends on what application the battery will be used for, either for power or energy delivery.

2.3.2 Stationary Batteries

Stationary batteries, sometimes also referred to as secondary batteries, are often used for emergency power and/or for uninterruptable power supply. These batteries have shallow cycle and usually left fully charged at all times during their lifetime with an occasional discharge that could happen when the main power source goes out.

Due to the reliability of the LABs, it is commonly used as a stationary battery in large buildings, hospitals and other areas where power supply cannot not be cut off.

2.3.3 Deep-cycle Batteries

These types of batteries discharge large amounts of their energy, typically over 80% to be considered a deep-cycle battery for at least several thousands of cycles. Several design modifications have been made in LABs in order to perform well in a deep-cycle environment, some of these modifications are to increase the space between the electrodes, increase the size of the electrodes, and added volume to the bottom of the battery to avoid damage from potential deposition of $PbSO_4$ particles which could affect the electrodes causing a short-circuit and ultimately premature failure.

2.3.4 Flooded Batteries

Flooded batteries, also referred to as “wet cells” are the most common batteries currently in the market. These are similar to the battery that Gaston Plante designed where the electrolyte is liquid, it is not sealed and the gases do not recombine with the liquids within the battery when recharging. Due to this, the battery requires maintenance by verifying water levels and making sure the battery is not trapping any gases that could cause an incident.

2.3.5 Sealed (SLA) / Valve Regulated Lead Acid (VRLA) / Absorbed Glass Matte (AGM)

As the LAB was improving, many versions and names for the batteries were given. The first sealed battery was developed in the 1970s, which was maintenance-free. This type of battery did not require watering and could be used in any orientation, it contained less electrolyte than a flooded type.

The Valve-Regulated Lead Acid batteries (VRLA) has the ability to combine oxygen and hydrogen to create water and prevent drying conditions during cycling. In addition to that, the absorbed glass matte (AGM) also emerged which is where the electrolyte is absorbed by the separators where the battery won’t spill anymore.

2.4 LAB Problems and Drawbacks

Unfortunately, the LAB also comes with some problems and drawbacks due to the nature of the materials used and chemical properties related to the use of lead. Such concerns are addressed in the following sections.

Lead is a heavy metal with a large atomic number, therefore its usage independent of its application, is linked to high weight systems. A good example of heavy weight systems, are

secondary batteries that are used as a backup energy source. Although extremely reliable when they are needed, they are heavy and need a large space to be in storage.

One of the major causes of failure in LAB is due to sulfation.[13] This happens when the battery is discharging and both plates crystallized to $PbSO_4$. Failure due to sulfation becomes an issue when the crystals formed during the chemical discharge become too large that it short-circuits the electrodes. Sulfonation tens to occur during deep cycles, sometimes the thickness of the $PbSO_4$ grows too much preventing the recharging process, current applied to the battery is no longer enough to reverse the material and in essence the battery cannot be effectively charged.[14]

Some of the effects of sulfonation are related to loss of capacity, loss of voltage, an increase of internal resistance and decrease in the concentration of sulfuric acid.

A method to counteract the negative effects of sulfation is to immediately recharge the battery after use. Batteries that go through this have high internal resistance and will only be able to deliver a small fraction of what it was rated to discharge current. This also affects the charging cycle, which will take longer to recharge therefore becoming less efficient.

There are many concerns regarding lead in the industry due to being a carcinogen and many industries have taken steps to lower the lead footprint used in paints and fuels to mention some. Due to unsafe practices, long-term exposure even through a small percentage of these materials can cause irreparable damage to the brain, kidney, hearing and even learning problems in kids.

Attempts to mitigate the issue have been ongoing for years and new methods for disposals and lead smelting are ongoing. In the past couple of years, improvements on recycling LABs have been extremely successful. For example, it was reported in the Battery Council

International that approximately 98% of all lead found in LABs was recycled between the years 2007 – 2011.[5]

2.5 Lithium-Ion Batteries (LIBs)

Fast-forward approximately 120 years, the lithium-ion battery was developed. It was first proposed in the 1970s by British chemist M Stanley Whittingham who was working at the time with Exxon. Whittingham proposed using titanium (IV) sulfide and lithium metal as electrodes for his battery, although it was rechargeable it was an impractical design due to hazards it created. Titanium (IV) Sulfide had to be synthesized and to be completely sealed and at the time it was being made it cost approximately $1000 per kilogram in raw material. When the material was exposed to air it would react and form hydrogen sulfide, H_2S, which is an extremely toxic gas. Due to this the development of the titanium sulfide lithium-ion battery was discontinued. Even without the titanium sulfide, the use of lithium was a challenge of its own. When using lithium electrodes, safety issues became apparent due to its high reactivity. Lithium burns at ambient conditions due to its spontaneous reactions with water and oxygen. Due to this, researchers focused their efforts in developing batteries where instead of just using lithium metal, lithium compounds were considered. These compounds were still capable of accepting and releasing lithium ions throughout the charge/discharge of the electrodes.

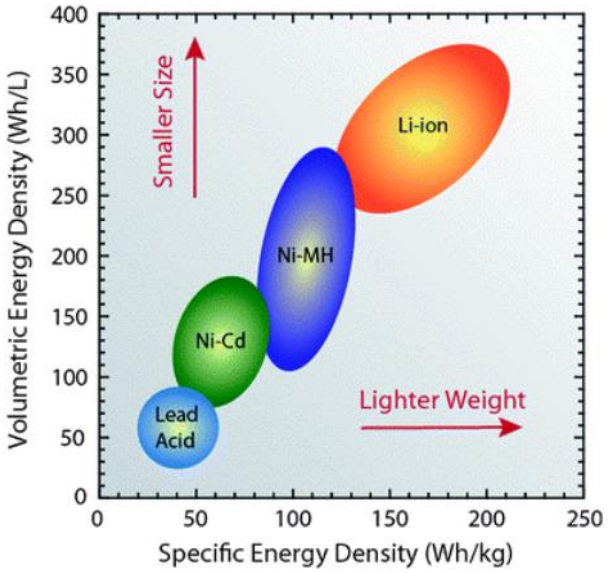

Figure 3 – Diagram of the specific energy density and volumetric energy density of the most common batteries in the industry.[15]

Lithium is an attractive material to use due to being a high electrode potential for having a low atomic mass, with high power/charge to weight potential and high energy density. Figure 3 shows how well Lithium-Ion batteries stand relatively LIB is generally constructed very similarly to LABs, which can be broken down in three main components: Electrodes, Separators and Electrolyte.

The electrodes consist of a positive and negative electrode. Typically, the positive electrode is made out of a metal oxide and the negative electrode of a composite with carbon. Currently the most commercially popular negative electrode material is graphite. Graphite is a favorite due to its mechanical and electrical properties.

Separators similar to the separators in LABs, have the purpose of separating the electrodes from physically touching each other and avoid short circuiting as well-being porous for the ions to can transfer from the electrodes with the electrolyte during the electrochemical process. Common materials used to create separators have ranged from simple microporous

polymer membranes to engineered polymers membranes. Changes have occurred due to the need to design separators as thin as possible to minimize the weight and volume within the cell and battery. Figure 4 represents a basic schematic of a LIB.

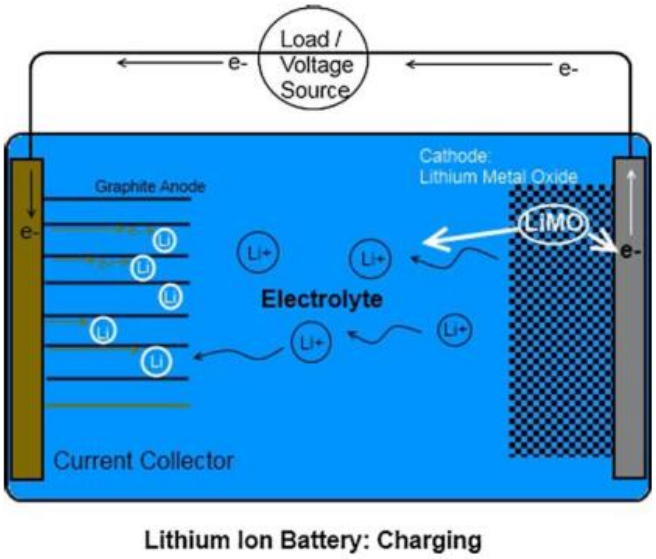

Figure 4 – Schematic of a lithium ion cell.[16]

The electrolyte used in LIBs is usually a mixture of organic carbonates such as ethylene carbonate or diethyl carbonation, which contain a variety of lithium ions. Also, non-liquid electrolytes are used, such examples are lithium triflate ($LiCF_3SO_3$), lithium tetrafuoroborate ($LiBF_4$), lithium perchlorate ($LiClO_4$), lithium hexafluoroarsenate monohydrate ($LiAsF_6$) and lithium hexafluorophosphate ($LiPF_6$).

2.6 Types of Lithium-Ion Batteries

Like LAB, there are many types of LIB in the market, each battery performs better in different types of environments. The following section will cover the most common types of LIB and the conditions under these works most efficiently.

Handheld electronics are mainly based out of lithium cobalt oxide ($LiCoO_2$) that is designed to offer high energy density with very stable capacities However, one of the main drawbacks of this type of battery is it susceptibility to thermal runaway, overcharging and safety hazards, especially when it is damaged.

Lithium Manganese Oxide ($LiMn_2O_4$) (LMO) batteries offer less energy density than lithium cobalt oxide but have a longer life expectancy and reduced probability of having catastrophic failures. One of the ways to mitigate these issues is through the exploration of different methods of production of the material, in one case it was studied how processing parameters in electrospinning (nanofiber making method) and the use of a polymer as a precursor resulted in an increased in surface area, which provided a shorter diffusion path for lithium ions and prevented self-aggregation which resulted in excellent high rate capability and cycling performance.[17]

Another study conducted with electrospinning lithium manganese oxide nanoribbons showed higher surface area and presented lower amounts of impurities when compared with nanoparticles.[18] In addition to nanoribbons, LMO nanotubes (NT) have been also synthesized and explored where it can have a capacity retention of over 98% after 100 cycles with an excellent high-rate capability; this is due to the hollow structure and network structure of the one-dimensional NTs which allows for a reduced diffusion distance for Li-ions.[19]

There has been publications regarding the possible use of lithium and lead.[20] A particular study conducted in 2002 in the University of Cordoba in Spain, tests done with lithium and different concentrations of lead and lead oxide were performed. When these samples were tested, in all samples the specific capacity when cycling decreased dramatically compared to how the

material started and did not improve until other additional processes added into the material improved the batteries performance.[21]

Since then, there has not been many studies conducted in the lab regarding lead and lithium testing. An article by Cheol-Min Park *et al*, did a broad study on lithium alloyed based anodes materials for Li secondary batteries and summarized that although Pb can theoretically can accommodate lithium up to $Li_{17}Pb_4$, it has not gathered enough attention due to the possible toxicity of Pb.[22]

The following year, Liwen Ji *et al* found that although Li can be electrochemically alloyed with Pb, the main challenge for these anodes was the large volume change during the Li alloying/dealloying processes.[20] Due to the large volume changes that the anodes go through, it experience severe cracking and crumbling which causes the battery to experience irreversible capacity. Some of the strategies that the study reported that have been investigated in order to mitigate the large volume change and keep the structural integrity of the anode has been through the addition of nanostructures, the addition of a second component to form a nanocomposite or the formation of an alloy to absorb the volume change. When discussing the second approach of addition a second component, the addition of carbon was used as an example which showed that the carbon matrix could act like a buffer for the volume change and with its good electrical properties improve the electrical conductivity as well the suppression of the formation of the SEI layer.

2.7 LIB Problems and Drawbacks

A major concern regarding LIBs is the instability of metallic lithium and the high energy density that it has when it becomes unstable. When LIBs were being developed, one of the major

challenges was the prevention of a thermal runaway during the charging period. Thermal runaway occurs when an increase of temperature charges the dynamics within the batteries increasing operating temperature beyond its melting point and eventually resulting in a destructive reaction. In order to mitigate this issue, researchers began exploring other types of electrodes minimizing the amount of active metallic lithium material to potentially increase safety in LIBs.

2.7.1 Metallic Lithium

Lithium in this state is extremely dangerous, it will ignite and burn when exposed to oxygen and has the potential of exploding when exposed to either air or water. Due to this issue, research has been geared towards replacing metallic lithium into lithium compounds that have the ability to release/accept Li-ions in order to perform the chemical reaction that discharges/charges a LIB. These new lithium compounds have significantly increased the safety of LIB.

2.7.2 Dendrites

Dendrite growth presents a safety concern in batteries.[23] When dendrites accumulate, the probability of piercing the separator increases causing short-circuits between the electrodes and potentially leading to thermal runaway. The formation of dendrites take place over time through various charge/discharge cycles and when the battery is cycled at a fast rate. When this happens, lithium fibers or “wires” form and start growing until the separator is pierced and short circuits the battery.

Thermal runaway takes place after dendrites accumulate and over time pierces the separator. This process continues until it combusts or explodes.[24–26] A potential reason why smartphones have been spontaneously combusting is because thermal runaway is taking place within the battery due to the accumulation of dendrites.[27]

2.8 Carbon

In the past couple of decades, many studies have evaluated the mechanical and electrical properties of carbon within LAB and LIBs.[28–36]

Moseley *et al* presented in a short communication how carbon enhanced the performance of LABs. Figure 5 show a variety where carbon has been used in different areas of the battery, such as grid and paste where it can serve as active material for the battery.

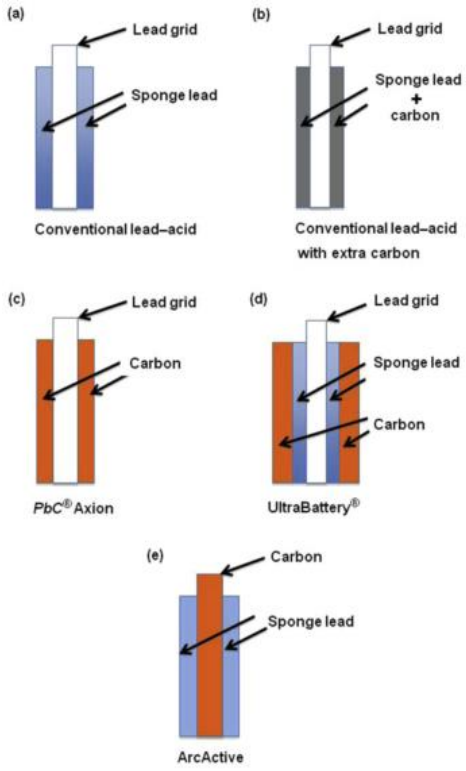

Figure 5 – Types of LAB configurations with carbon.[37]

These studies have shown that there is evidence to suggest there are at least three ways that the addition of carbon can change the performance on a LAB which are 1) capacitive contribution, 2) increasing the surface-area where the electrochemical processes can take place the physical process.[37]

In LIBs, it has been found that carbon allows to construct flexible electrodes which would expand the type of environment that the battery can be exposed without being easily damaged.[38–40]

Activated Carbon is a type of carbon that has been processed to have a large surface area therefore facilitating chemical reactions and/or absorption-desorption. A study conducted in North Carolina in 2009 explored how activated carbon nanofibers performed in a LIB.[41] Results showed that the electrochemical behavior of such anodes presented improvements in the lithium-ion storage capability and better cyclic stability when compared to the inactivated materials. Additional studies collaborate with similar findings that activated carbon exhibits higher efficiency and rate of performance when incorporated into the material.[42]

Graphite, an allotrope of carbon has been increasingly used in batteries for the past couple of decades. It is commonly used for LIBs in portable electronics and electrical vehicles. In LIBs, it has been shown to deliver lower-cost and safer batteries when compared to the usage of metallic lithium. It was found that when natural graphite was used it exhibited a high reversible capacity and high coulombic efficiency. It was also noted that that even though it has a better performance when it goes through high-rate discharge, it has a poor performance at low temperatures because the low diffusion of the lithium to the graphite.[43]

Graphite is also used in LABs, Fernandez *et al.* investigated when graphite is added to the negative added material to the electrode.[44] The battery was tested until failure without the

addition of graphite and observed that lead sulphate tends to accumulate on the outer part of the plate which created a dense layer which prevented the electrolyte from properly reaching the active material of the electrode. When graphite was added to the active material of the negative electrode, it was found that lead sulphate was generated while the battery is discharging; but the lead sulphate was distributed evenly along the thickness of the plate which did not inhibit the electrolyte from the active material.

Graphene is a form of carbon consisting of a single layer of atoms that is arranged in hexagonal lattice. When used in LABs, it has been found that graphene increases the surface area and has a great electrical conductivity from where the graphene was mixed with the graphite nanopowders and increased the recoveries were acceptable and ranged from 65.8% to 113.5% for Lead.[45]

Polyacrylonitrile (PAN) is commonly used as a precursor of choice when carbon fibers will be needed for high performance characteristics. A recent study conducted at the University of Texas – Rio Grande Valley investigated polyvinyl alcohol (PVA) and polyvinyl butyral (PVB) as potential low cost precursors for the production of carbon fine fibers.[46,47] After the material was spun into fibers, these were subjected to a dehydration process by being exposed to sulfuric acid vapors. Once the mats were partially carbonized, the sample was calcinated to 850°. The developed nonwoven mats demonstrated promising electrical properties (i.e. high shielding effectiveness of electromagnetic interference) coupled with mechanical integrity therefore making these membranes promising for electrochemical applications.

2.9 Nanotechnology

Nanotechnology has changed the way materials are looked and developed when creating materials down to the nanoscale. Through these improvements, processes and applications have

revolutionized how items are now created. In battery applications, the use of nanotubes, nanowires and nanofibers to name a few have been deeply investigated.

Specifically, carbon nanotubes have shown to be valuable for LAB. Carbon nanotubes have excellent electrical and thermal conductivities, mechanical flexibility and significant large surface area. Studies conducted, for example by Swogger *et al*, show that discrete carbon nanotubes (dCNT) uniformly dispersed in the battery negative paste increase the charge acceptance of the LAB by over 200% and reduce energy losses by more than 15%.[48] In a different study from the same group, the effect of dCNT in battery performance was evaluated upon adding these to both electrodes. By doing so, the addition of the carbon nanotubes showed no effect on the past density, it increased the cycle life to over 60% and decreased the water loss per cycle by over 19%.[49]

Adding carbon nanotubes to the negative added material or positive added material, has shown signs of enhancing conductivity which aids in avoiding sulfation along the electrodes and prolongs the cycle-life.[50]

For LIB, carbon nanotubes have shown significant improvements when use as additives in the electrodes. [51] Studies conducted at Florida International University have shown that when carbon nanotubes are added as alternative anode materials, either as an allotrope of graphite or a composite, it can alleviate the degradation of the electrode which has a significant volume change with charging and discharging process.[16]

Over the years the development of spinning processes in producing fibers have been evolving to where it is possible to manufacture fibers with diameters of a few nanometers to few hundred of nanometers. The types of spinning can be summarized into the following: wet spinning, dry spinning, melt spinning, gel spinning, electrospinning and forcespinning®.

Wet spinning is considered the oldest fiber manufacturing method. In order to produce the fibers, the spinneret is submerged in a chemical bath which causes the fiber to precipitate and solidify.[52] These fibers can be collected either as continuous tow or rope.[53] One of the drawbacks of using wet spinning relies on the inability to obtain nano or submicron scale fibers at industrial yield.

In the case of dry spinning fibers are produced upon evaporation of the solvent which typically occurs under a stream of inert gas or air. The benefit of using dry spinning over wet spinning is not having to dry the fiber.[54]

In the case of melt spinning, fibers are directly produced from the polymer without the need of a solvent, mostly toxic organic solvents, this process results in significant savings given the absence of the solvent and costs associated with solvent recovery steps. The process is usually performed through extrusion of pellets or granules from a solid polymer which are shaped into fibers.[55]

Most of the reports found in the literature use the electrospinning technology for the development of nanofibers. This technology was developed in the 1930s, but became attractive for nanofiber development in the early 90s.[56] Electrospinning works through the use of an electric field to create a charged jet on a polymer solution.[57] The setup for electrospinning consists of three major components: a high-voltage power supply, a spinneret and a collector.[58] The production of fibers happens when the spinneret is connected to a syringe that contains the solution that will be made into fibers. The solution is fed through the spinneret at a constant rate and when a high voltage, anywhere from 1 to 50kV, is applied; the surface of the solution out of the nozzle will become electrified. After the strength of the electric field overcomes the surface tension of the solution, it forces the solution out of the nozzle. When the jet of charged solution

travels through the air, the solvent evaporates and leaves behind a charged fiber that can be collected. The fibers produced from this method can range from a couple of hundred micrometers as small as a few tens of nanometers.[59,60] Several studies have developed lead based nanofibers using the electrospinning process, in particular studies involving perovskite lead zirconate titanate (PZT) based materials.[61,62] N. Dharmaraj *et al*, synthesized and produced lead zirconate titanate nanofibers in the range of 200 – 300 nm.

In order to address the production quantity of fibers developed by electrospinning, the use of centrifugal force spinning resulted in a novel method called Forcespinning® to create fine fibers. [63] This technology replaces the need to use an electric field of which bring benefits of increasing the materials choice to be produce into fibers, improves the production rate and reduces the cost of operation.

Forcespinning machine are the following: spinneret, thermal system, collectors, control system, chamber, motor and a break, detailed information about operating conditions and diagrams can be found on found on Chapter 3 Section 2.

In the literature review conducted, there has not been any research conducted in the development of the lead nanofibers for battery applications. As mentioned earlier, the potential for studying the material was not looked into due to its toxicity and the hazard it can be to the environment. However, with new breakthroughs that has been found recently through nanotechnology in current applications and the limitations that lithium will bring in the future, it is important to explore the production of lead-based nanofibers and its performance on a lithium-ion battery. The ability to produce nanofibers could promote the usage of lead but at much lower quantities therefore decreasing the hazardous effects while improving performance.

CHAPTER III

EXPERIMENTAL SETUP

3.1 Introduction

This chapter discusses the experimental setup that was used to produce and collect the data that is presented in this thesis. A description of all the equipment used is provided along with their application for nanofibers development/characterization and battery fabrication.

3.2 Fabrication Equipment

3.2.1 Magnetic Stirrer with Hot Plate

A magnetic stirrer with hot plate was used to mix the solutes and solvent into a homogenous solution for pre-determined about of time. Temperature throughout the mixing process was kept constant.

3.2.2 Forcespinning Cyclone

Until recently, the most common technique to produce nanofiber fabrication was through electrospinning but it came with a material production drawback and the electro hazard on operating on voltages from 1 to 50 kV. The Cyclone from Fiberio Technology Corporation addresses that issue by producing the amount of fibers produced by electrospinning in a day by as little as a few minutes

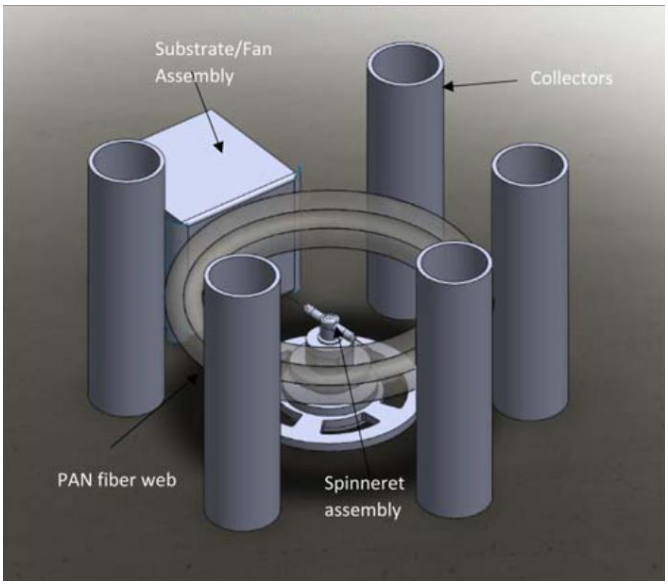

Figure 6 – Schematic drawing of a typical setup inside the Cyclone showing the spinneret, collectors, fan assembly.[64]

3.3 Characterization Analysis

3.3.1 Scanning Electron Microscopy (SEM)

The SEM images were obtained by using a Zeiss SEM. The scanning electron microscope consists of a column and the cabinet.[65] Figure 7 shows the column is the area where the electrons travel from the emission until it interacts with the sample and where the detectors are installed to capture the signals that results in the behavior of the electrons and the sample. The detectors will transform the signals into an electrical signal which will be sent over to the cabinet for processing that can be presented as images and/or graphs.

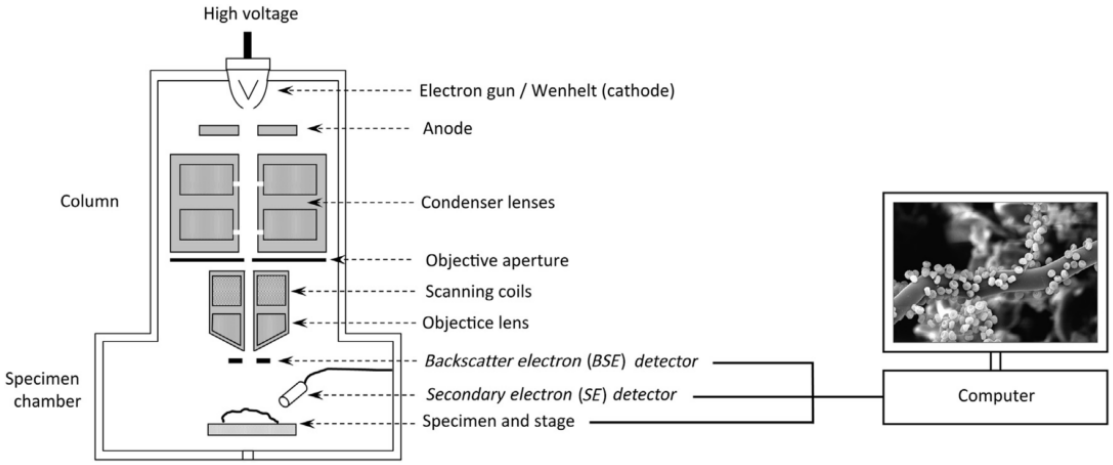

Figure 7 – Schematic representation of an SEM.[66]

This is a type of electron microscope that produces a series of images by scanning the surface of the sample by a focused beam of electrons also known as primary electrons (PE). These electrons once they interact with the atoms with the sample provide information that can be used to get information regarding its morphology, structural organization & chemical composition in the form of secondary electrons (SE), backscatter electrons (BSE), auger electrons (AE), characteristic X-rays, bremsstrahlung X-rays, cathodoluminescence (CL, visible light) and heat. [65] Images generated by the electron microscope can have magnification of over 100KX.

SEs are a result of the inelastic scattering of PEs that have a low energy, 3-50 electron volts (eV). Since these possess low energy, they are usually collected and amplified by means of an Everhart-Thornley detector, which is a combination of a scintillator and a photomultiplier.[67] Once amplified, the resulting signal is proportional to the amount of SE collect. With these signals it is how an image is generated.

BSEs are done by elastic scattering of PEs when it interacts with sample atoms. Because these electrons have about 60-80% of the energy from the PEs, they are able to escape from the region of the interaction volume. This signal is how it can be determined what type of material the sample is and generate topography-sensitive signals.[67]

Figure 8 – Zeiss SEM used to characterize the fibers.

Auger electrons are a relatively low energy signal that is generated by the creation when electrons are knocked out of the inner electron shells due to the collision of PEs into the sample. Since AEs have low energies it can only escape a few nanometers away. The cathodoluminescence signal can be used as a signal for image formation as well as the secondary electrons.[67]

3.3.2 Energy-dispersive X-ray Spectroscopy (EDS)

The EDS analysis was conducted within the Zeiss SEM by a pre-mounted EDS. The sensor picked up the backscattering electrons from the electrons focused in the sample. Through

this, it is possible to having an elemental analysis through the fundamental principle that each element has a different atomic structure of which are plotted on an electromagnetic emission spectrum.

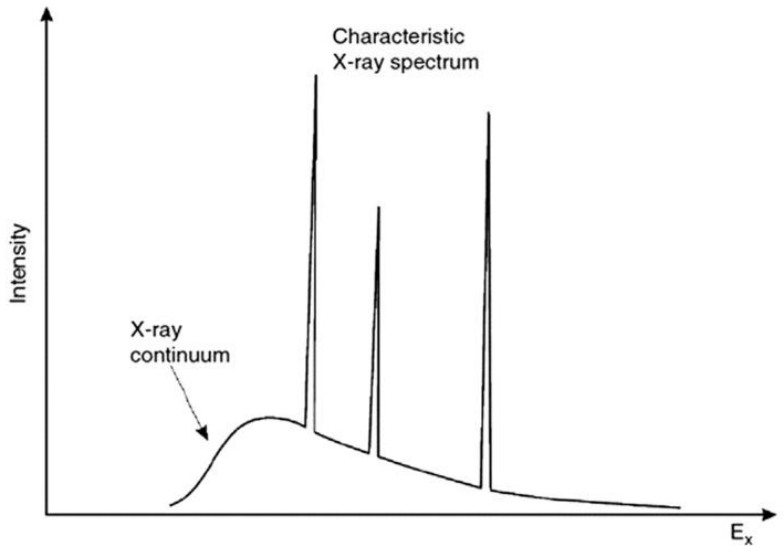

Figure 9 – Schematic representation of the EDS spectra.[68]

All elements have a unique set of peaks throughout this spectrum of which it is used to determine what elements are contained within the sample. These peaks are generated upon the interaction between the electrons from the SEM and the nucleus of the atoms in the sample.[68]

3.3.3 Thermogravimetric Analysis (TGA)

A TGA is a thermal analysis of which the mass of the sample is measured as a function of temperature. The results can be plotted against temperature or time of which will show the mass changes.[69] There are three types of analysis that the TGA can perform: dynamic, isothermal and quasistatic.

The dynamic (also known as the constant heating rate) approach is based on the equation on figure 10, where Ea is activation energy (J/mole), R is gas constant (8.314 J/mole K), b = constant, β = heating rate (°C/minute) and T = temperature of weight loss (°C).

$$Ea = \left(\frac{-R}{b}\right) \frac{d\ 1n\ \beta}{d\left(1/T\right)}$$

Figure 10 - Constant heating rate equation.[70]

Figure 11 – TA Model 400 used to analyze fibers.

There are several different ways or reactions that can cause for the sample to experience a mass change, which can either be a decrease or increase in mass through phase transitions, absorption and desorption. These can include evaporation of volatile constituents, oxidation of metals, oxidative decomposition of organic substances, thermal decomposition, heterogeneous

chemical reactions and ferromagnetic materials where the magnetic properties of some materials change with temperature.[69]

3.3.4 X-ray Photoelectron Spectroscopy (XPS)

To evaluate the composition of the surface of a sample, it will be necessary to use the XPS. The XPS is a quantitative spectroscopic technique that measures the elemental composition of the samples at the surface and a few levels right before the surface. The spectrum with a series of photoelectron peaks is obtained by shooting a beam of X-rays while measuring the kinetic energy and number of electrons that leave the sample from the surface down to 10 nm deep. This technique is specific to surface due to the short range of the photoelectrons that are excited from the sample.[71] Each element has a unique binding energy peaks that determines what the sample is composed of. The XPS is also able to provide the chemical bonding information as well due to the shape of each peak and the binding energy that it altered by the chemical state of the atom.

Figure 12 - The XPS was used to measure the elemental composition of the fibers.

3.4 Electrochemical Analysis

3.4.1 Cycle Performance

A charge cycle is the process where a rechargeable battery is charging and later discharged into a load. This is done to quantify the battery's expected life. These tests might vary given to how much the battery is required to be discharged. Typically, the number of cycles that a rechargeable battery is rated for is either for how many times it can go through the process or begins to lose its capacitance.

The electrochemical performance was evaluated by carrying out a galvanostatic charge – discharge experiments at a current density of 100 mAg^{-1} and 200 mAg^{-1} between 0.05 and 3.0V. Due to the different mass of the anodes, the specific charge/discharge capacities were calculated based on the mass of the nanofiber anodes.

3.4.2 Cyclic Voltammetry (CV)

To have an understanding of the electrochemical reactions within the battery, a cyclic voltammetry test is needed. The behavior of the CV curve will also be indicative of what type of materials are interreacting within the cell. If peaks or valleys happen throughout the test which was not expected, it could be indication of foreign material that contaminated the battery during assembly. These cycles are repeated as many times is necessary for the experimentation to study the electrochemical properties of the anodes.[72]

The cyclic voltammetry was conducted using an electrochemical impedance spectroscopy (Autolab 128N) with a scan rate of 0.1 mVs^{-1} to analyze the anodes.

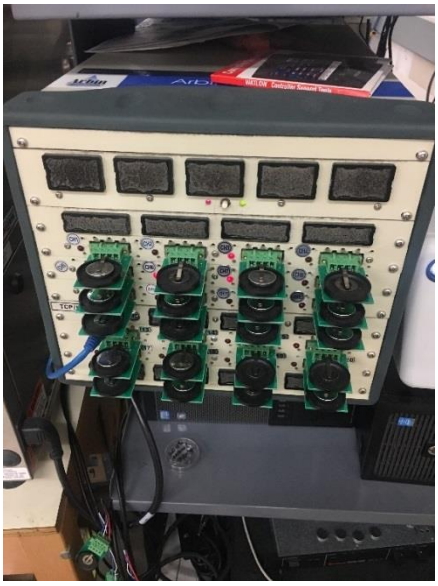

Figure 13 – Battery load station to the Autolab 128N

3.4.3 Rate Performance

The rate performance test involves in charging/discharging the battery at increasing rates through a period of time and then charge back at its initial charge/discharge rate and compare how much the quality of the charge is from its initial to what is currently charging. The parameters used for this thesis was 50, 100, 200, 400 and 500 and back to 50 mAg^{-1} for 10 cycles each.

This test allows to see how the battery will behave in different charging rates and if it reverts back to its initial performance before experiencing different types of charge/discharge rates.

CHAPTER IV

EXPERIMENTAL PROCEDURE

4.1 Materials Used

Polyvinyl Alcohol (Kuraray, POVAL 27-96, 96%), Lead (II) Acetate Trihydrate (99+%, Acros Organics), distilled water, Lithium metal, glass microfiber separators, 1 M LiPF6 salt in ethylene carbonate (EC) / dimethyl carbonate (DMC) (1:1 v/v) solvent and 2032 coin-type cells to perform the electrochemical tests.

4.2 Solution Process

Solutions were made in 10 mL scintillation vials with magnetic stirrers and sealed with parafilm to prevent potential solvent evaporation.

Lead Concentrations Used		
Lead Concentrations (g)	PVA Concentrations (g)	Distilled Water (g)
0.10	1.00	8.90
0.25	1.00	8.75
0.50	1.00	8.50
1.00	1.00	8.00
2.00	1.00	7.00
2.50	1.00	6.50

Table 1 – List of solutions used to spin into fibers

Figure 14 – A sample prepared in scintillation vials and sealed with parafilm prior heated oil bath.

Various of concentrations were made of Lead (II) Acetate to the PVA to find to optimal concentration needed to yield the maximum amount of fibers. The table below show which solution concentration was optimum.

Lead Concentration					
RPM	1%	2.50%	5%	10%	15%
3000					
4000					
5000					
6000					
7000					
8000					
9000					
10000					

Legend
Good
Some
No Fibers

Table 2 – Visual quantity of fibers produced when spinning 1 mL of solution.

1 g of PVA and 0.5 g of Lead (II) Acetate were added to 8.5 g of distilled water. Once the solutes and solvent were inside the scintillation vial along with the magnetic stirrer, the vial was sealed with parafilm. The vial was later placed inside a heated silicon oil bath at 80°C for four

hours while stirring at 400 rpm. After the solution has completed the time in the heated oil bath and became homogenous, it is taken out and it is cooled to room temperature and continue to magnetically stir overnight. This procedure was used by Cremar *et al*, when they successfully created nonwoven fibers produced by water soluble precursors.[47]

4.3 Fiber Production

After the solution was magnetically stirred overnight, it was taken over to the Cyclone system where it was placed to produce PVA-Pb fibers. 1 mL of solution was placed inside the spinneret with 30-gauge needles attached at the end of the spinneret.

Figure 15 – Cyclone L1000 used to produce the PVA-Pb fibers.[73]

Once the spinning cycle was completed, the unit was opened and a 3” x 3” aluminum square was used to collect the fibers into a uniform mat. 10-ml solution yielded eight runs in the Cyclone machine. Once the mat was collected, it was stored in an oxygen-free environment until the carbonization process was set to begin.

4.4 Carbonization Process

Prior to carbonizing the collected fiber mat, these were stabilized on an oven at 120°C for 24 hours at ambient atmosphere.

Figure 16 – Dehydration of mat prior carbonization.

After the dehydration process, the sample was carbonized the GSL – 1700X oven. The sample was placed in the middle of the ceramic crucible where the heat will be at its highest efficiency once placed inside the oven. The carbonization process was carried out under an Argon atmosphere with a low rate of 80 ml/min to prevent further oxidation. The chamber was stabilized for 120 minutes at 50°C followed by heating up to 850°C at a heat rate of 3°C/min. Then sample was held at 850°C for 15 mins before cooling down to 500°C at a cooling rate of 3°C/min until the program is complete at 500°C. Once the furnace cooled to room temperature, the sample is taken out of the chamber and visually inspected to analyze the flexibility of the mat and potential for battery testing.

Figure 17 – GSL – 1700X used to carbonize PVA-Pb fiber mats.

4.5 LIB Assembly

The developed lead-doped carbon nanofiber mat was used an anode to evaluate in a lithium-ion battery and to evaluate its electrochemical properties. To build an Li-ion battery the following items were used; top terminal (+ positive), anode, electrolyte in separator, cathode, spacer, spring and a bottom terminal (- negative).

The electrochemical performance on the lead-carbon nanofibers anodes was performed using 2032 coin-cells. The weight of each anode ranged from 3 – 11 mg which were punched directly from the lead-carbon mat.

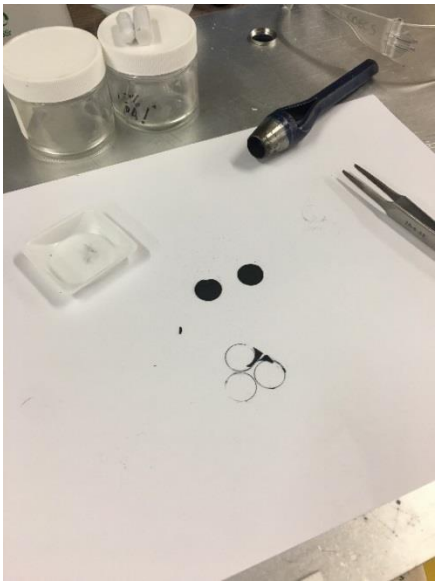

Figure 18 – Two Lead Carbon Anodes punches from carbonized mat.

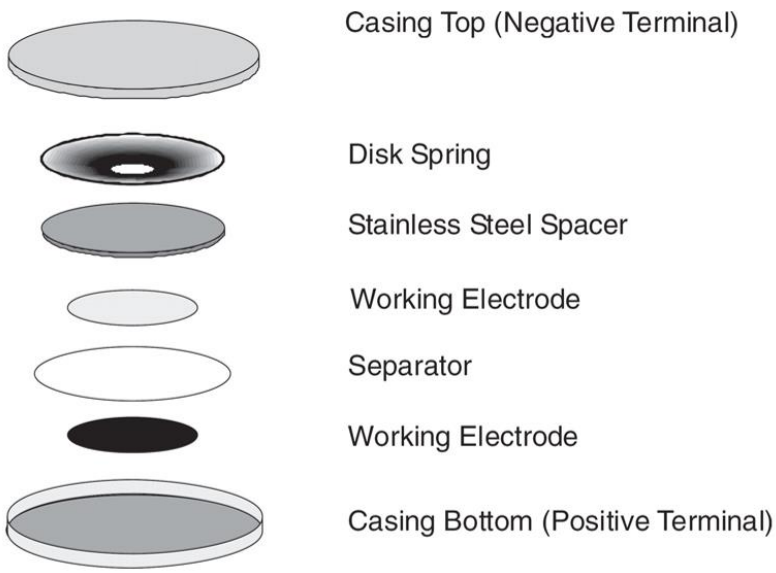

Figure 19– Half-cell lithium-ion battery assembly

The anode was used as a binder-free electrode, no additives were used. Lithium metal was used as a counter electrode, this is to keep the only variable when investigating the tests on the anode since there are plenty of studies conducted with lithium electrodes. Glass microfibers

were used as the separator. The electrolyte used was 1 M $LiPF_6$ salt in EC/DMC (1:1 v/v) solvent. The cells were assembled in an argon-filled glove box (Mbraun, USA) with O_2 and H_2O concentrations of <0.5 ppm.

When assembling the half-cell lithium-ion battery, the casing bottom is placed on a flat surface and we place our anode, which is the lead-carbon, inside. Then a separator is placed on top of the anode and a few drops of electrolyte is dropped on the separator. Once this is completed, a lithium metal cathode is placed on top of the separator. After the cathode was added to the battery, the final components of the battery were added which were the spacer, spring and bottom terminal then pressed at 1200 psi.

CHAPTER V

RESULTS & DISCUSSION

This chapter discusses the results that were obtained during the production and characterization of fibers and an electrochemical analysis in half-cell lithium ion batteries. At the end of the results section, a post mortem analysis was also conducted to see the integrity of the lead carbon fibers after 100 cycles.

5.1 Characterization

5.1.1 SEM

From the SEM images taken in Figures 20 and 21, the lead carbon fiber has a homogenous and continuous morphology

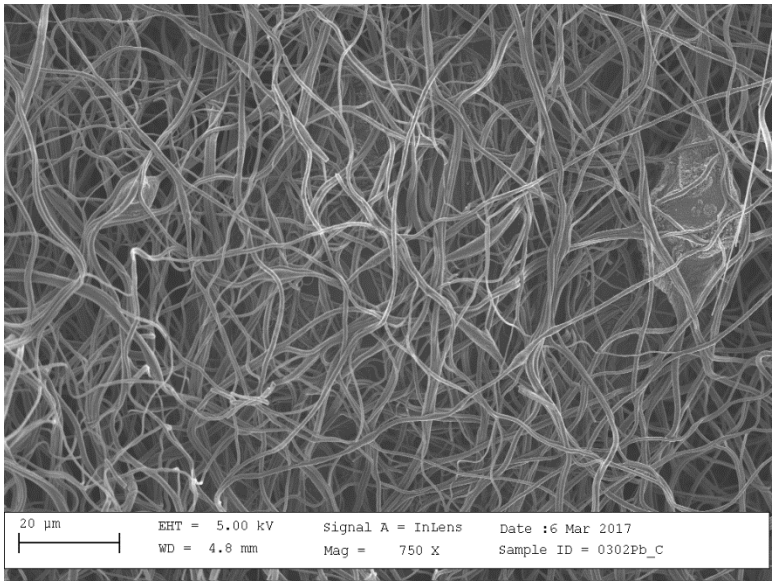

Figure 20 – SEM image from a lead carbon sample at 750X.

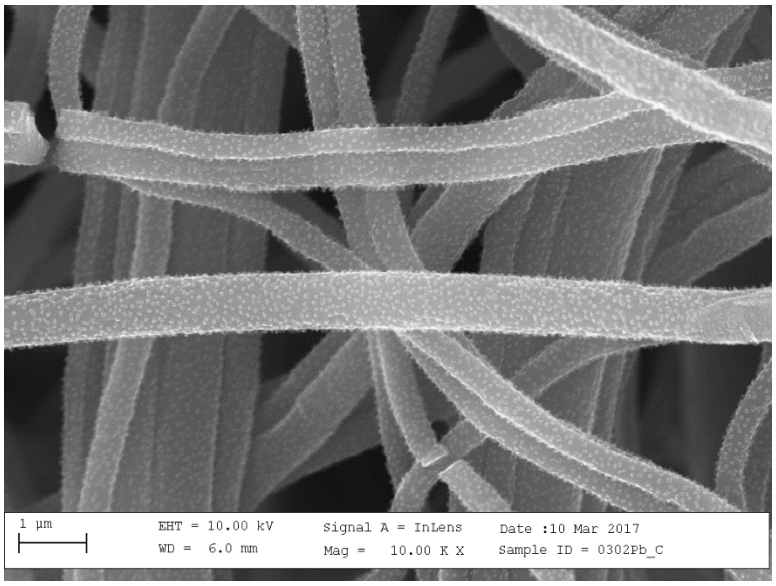

Figure 21 – SEM image from a lead carbon sample at 10KX.

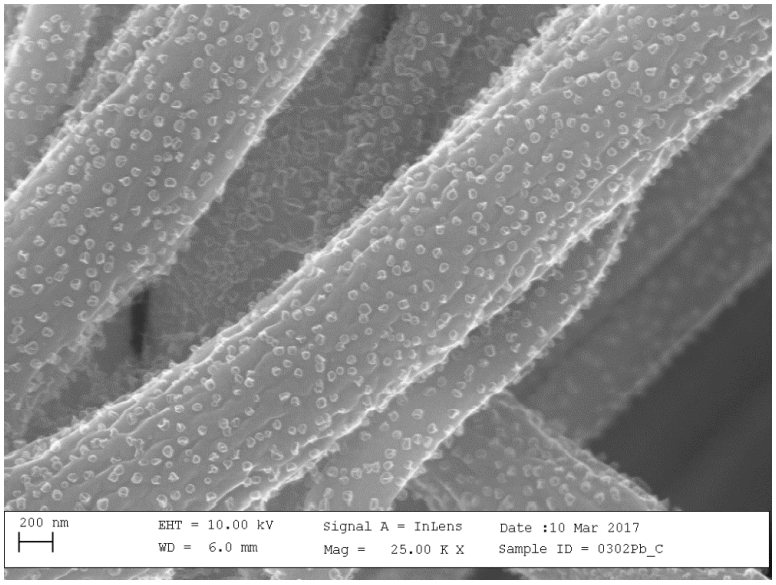

Figure 22 – SEM image from a lead carbon sample at 25KX.

Figure 22 show particulates scattered along the surface of the fiber. This resulted in lead particles as found by the EDS in the following section. The diameter of the fibers ranged from 250 – 750 nm.

5.1.2 EDS

An elemental mapping analysis was conducted on to analyze the material characteristics and to verify what type of substance was deposited on the surface of the fibers. Figure 24 represents the EDS spectrum shows three materials present in the sample; Carbon, Lead and Oxygen.

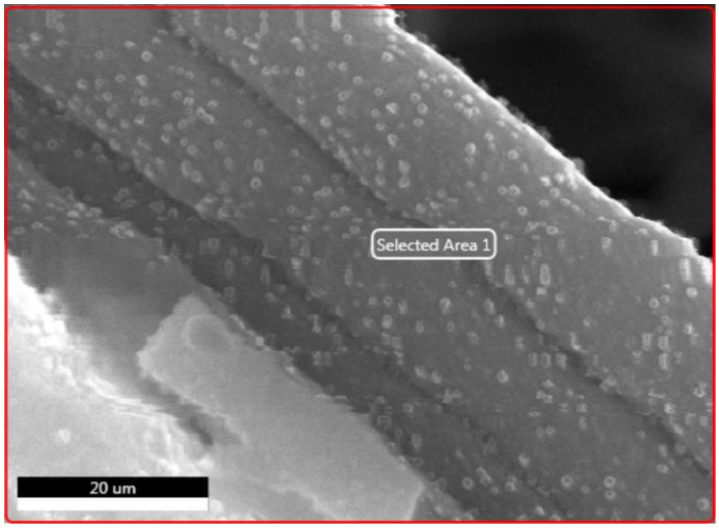

Figure 23– Section of the fiber analyzed with the EDS to determine material characterization.

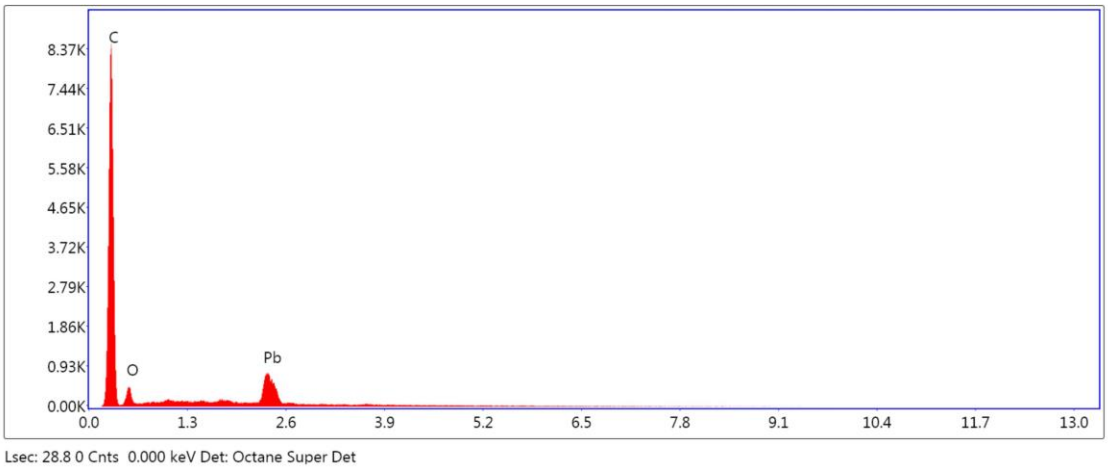

Figure 24 – EDS Spectra of the lead carbon sample in Figure 23

When the EDS focused solely into the granules found in the surface, it resulted to be mainly Pb as shown in the EDS spectrum on Figure 26.

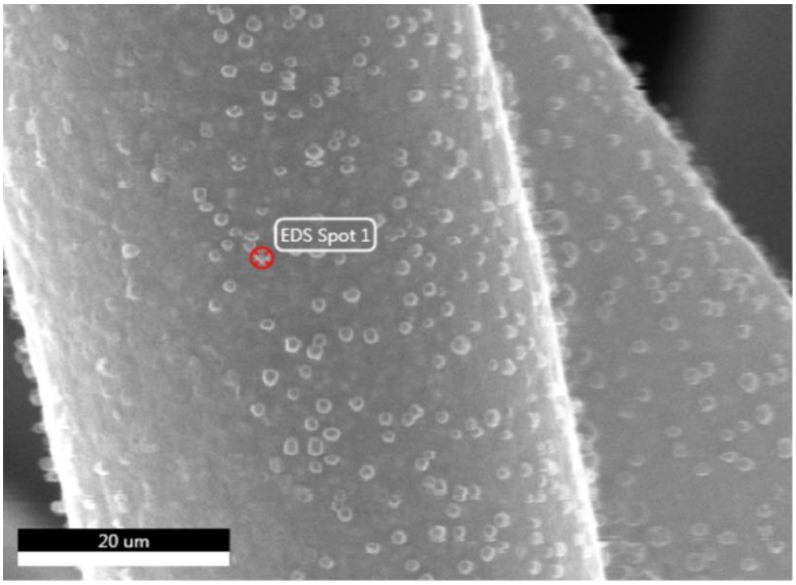

Figure 25 – Section of the fiber analyzed with the EDS to determine the material characterization.

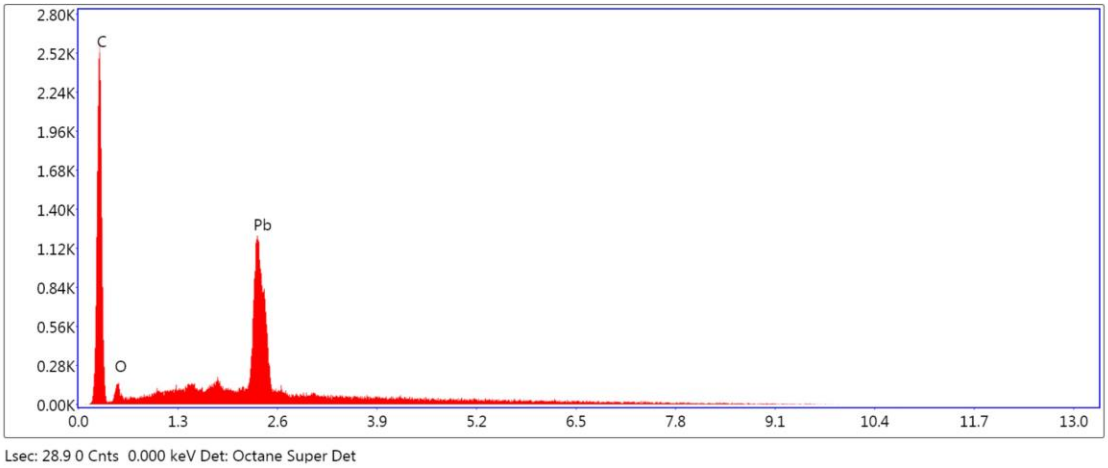

Figure 26 – EDS Spectra of the lead carbon sample.

An elemental distribution shown in Figure 27 where it illustrates the quantity of the material throughout the fiber, different colors are observed showing how the nanofibers are predominantly composed of 52% Carbon and 44% Lead.

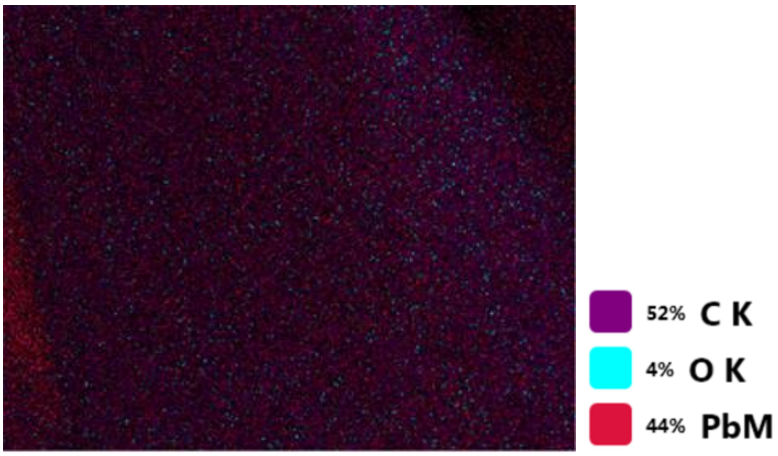

Figure 27 – EDS mapping of the lead carbon fibers showing a 44% Pb content distributed evenly among the fibers.

5.1.3 TGA

TGA analysis of PVA fiber only, PVA-Pb and Pb-C is shown on Figure 28. The analysis was performed in a nitrogen environment.

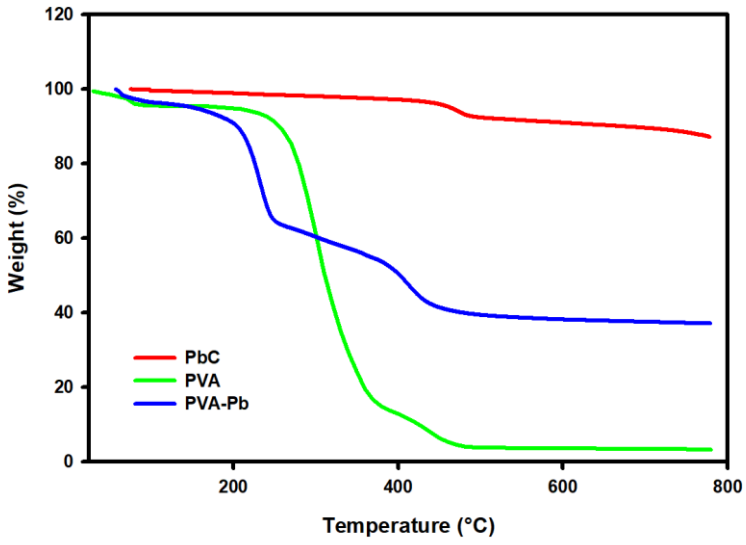

Figure 28 – TGA analysis of PVA, PVA-Pb & Lead Carbon fibers

For the PVA and PVA-Pb samples, it can be seen that approximately at 100°C there is a minor weight reduction, which corresponds to the removal of physically absorbed water from the

fibers. From the graph shown it can be seen how the PVA sample completely degrades after reaching 463°C and goes down to less than 5%wt by the end of the analysis. This result coincides with previous studies. On the PVA-Pb, which is the sample acquired right after spinning the solution into fibers and prior carbonization, between temperatures 152°C and 364°C there was multiple decompositions that could be attributed to the Poly(vinyl) Alcohol and Lead (II) Acetate. Lastly, the lead carbon nanofibers were shown to retain most of its weight by 88%wt as the analysis was complete.

5.1.4 XPS

XPS analysis shows the presence of lead at the surface of the fiber. The XPS data show the survey done with a large range where all three materials are shown with their respective binding energies. Figure 29 shows the XPS survey spectra the dominant peaks were those of carbon, lead and oxygen. (i.e. C1s, Pb4f and O1s) at binding energies of C1s and O1s at ~284.5 and ~532 eV, respectively.

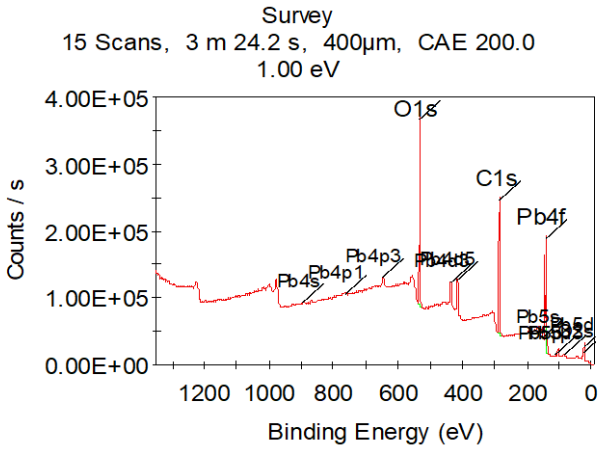

Figure 29 – XPS spectra showing spectra of C1s, O1s & various Pb in the fiber.

Figure 30 presents the range that is focused on the Pb binding energies; Pb $4f_{7/2}$ and $4f_{5/2}$ peaks are observed at 138.9 and 143.5 eV, respectively, correlates to what other studies have shown where Pb is bound to oxygen which indicates the presence of Pb ions on the fibers.[74]

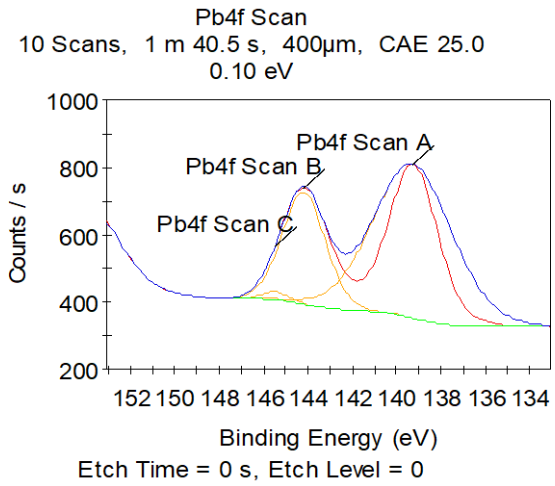

Figure 30 – XPS spectra of the Pb4f scan

5.2 Electrochemical Analysis

The following are the findings found when testing the Lead Carbon and Carbon anode batteries in the half-coin cells. The following three electrochemical tests were done to analyze the electrochemical performance of the batteries: Charge/Discharge, Cyclic Voltammetry and Rate Performance.

5.2.1 Cycle Performance

The electrochemical performance was evaluated at room temperature by carrying out a galvanostratic charge-discharge experiments at a current density of $100mAg^{-1}$ between 0.05 and 3.0V. Charge/discharge curves were obtained for the carbon and lead carbon anodes cycling at a current density of 100 $mAhg^{-1}$ from 3.0V to 0.05V. The carbon anode exhibited a high initial

capacity of 841 $mAhg^{-1}$ but quickly dropped to 272 $mAhg^{-1}$ by the following charge. The specific capacity of the carbon anode stays stable on the 10^{th}, 50^{th} and 100^{th} cycle at 204 $mAhg^{-1}$, 191 $mAhg^{-1}$ and 179 $mAhg^{-1}$.

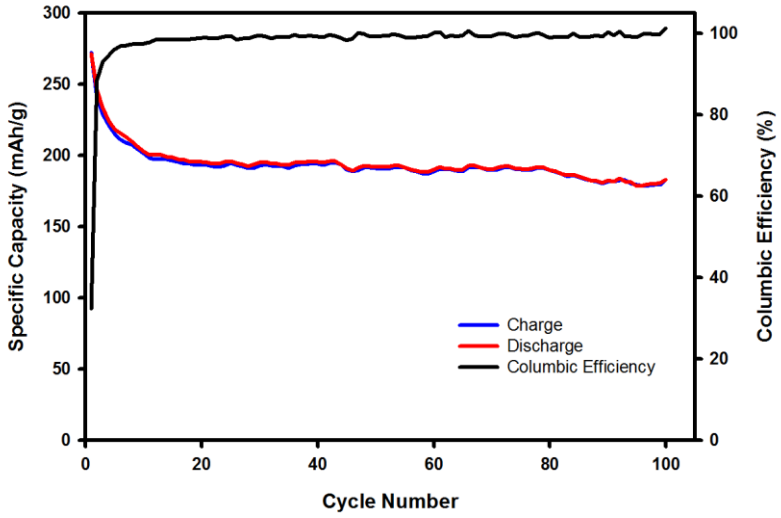

Figure 31 – Columbic Efficiency of the carbon fiber anode performed after 100 cycles at a current density of 100 mAg^{-1}.

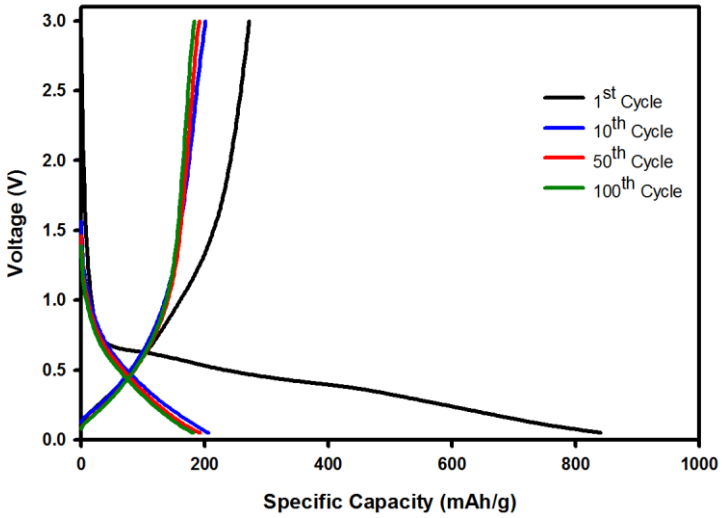

Figure 32 – Cycle Performance of the carbon fiber anode performed after 100 cycles at a current density of 100 mAg^{-1}.

Charge and discharge results on the lead carbon anode were higher compared to the carbon anode alone as shown in Figure 33. The lead carbon anode exhibited a high initial capacity of 612 $mAhg^{-1}$ and quickly dropped to 266 $mAhg^{-1}$ by the following charge. The specific capacity of the carbon anode stays stable on the 10^{th}, 50^{th} and 100^{th} cycle at 265 $mAhg^{-1}$, 277 $mAhg^{-1}$ and 270 $mAhg^{-1}$. Unlike the carbon anode, the lead carbon anode experienced a capacity recovery from early cycling. It recovered from the 10^{th} cycle to 50^{th} cycle from 265 $mAhg^{-1}$ to 277 $mAhg^{-1}$ and from the 50^{th} to 100^{th}, from 277 $mAhg^{-1}$ to 270 $mAhg^{-1}$, although it faded in specific capacity, the specific capacity of the 100^{th} cycle is relatively higher than the 10^{th} cycle the battery experienced during the test. The increase of capacitance during cycling could be attributed to the increase of reactive sites within the lead carbon anode allowing more Li ions to interact with the Pb and C.

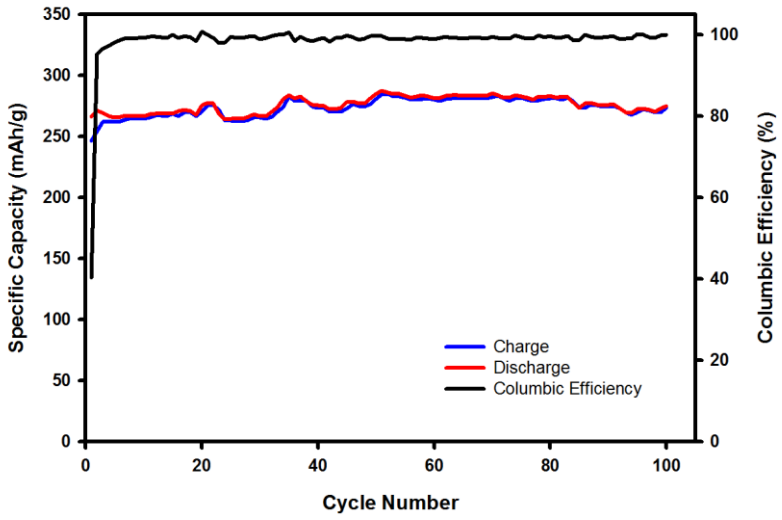

Figure 33 – Columbic Efficiency of the lead carbon fiber anode performed after 100 cycles at a current density of 100 mAg^{-1}.

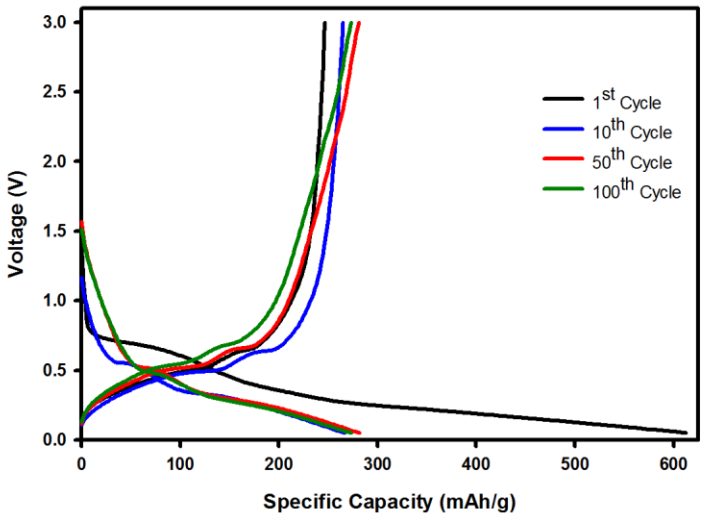

Figure 34 – Cycle Performance of the lead carbon fiber anode performed after 100 cycles at a current density of 100 mAg^{-1}.

When compared to carbon anode LIBs, the performance of the lead carbon nanofiber anode had 51% higher specific capacity than the carbon anode when tested on a half-cell lithium-ion battery.

5.2.2 Cyclic Voltammetry

In order to have an understanding of the interaction of lithium on the carbon and lead carbon anode, cyclic voltammetry were conducted on both batteries. As shown in Figure 35, there is a broad peak in the first cycle. This is due to the formation of the solid electrolyte interphase (SEI) layer. Irreversible reactions occur during this first discharge at the surface of the electrode and the remaining cycles do not have any more irreversible reactions and have reversable reactions. The chemical interaction that is happening between the lithium and the carbon anode intercalation and deintercalation of Li ions in the carbon. The chemical reactions involved in the half-cell can be described as the following equation:

$$6C + xLi^{+} + xe^{-} \leftrightarrow Li_xC_6 \ldots(1)$$

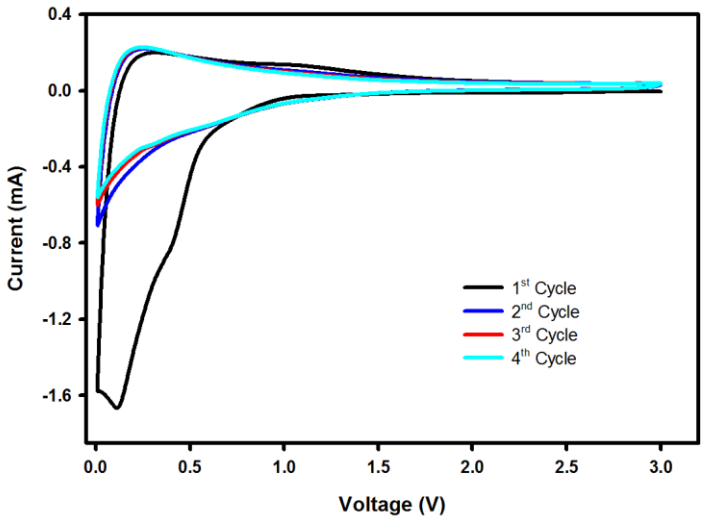

Figure 35 – Cyclic Voltammetry of carbon fibers between 0.01 and 3.0 V at a scan rate of 0.1 mVs^{-1}

In the lead carbon anode, as shown in Figure 36, does not experience such a large irreversible reaction due to the SEI layer. However, four peaks are recorded after the second cycle, two while discharging and two while charging. These peaks also appear on cycle three and four. This reaction is due to the alloying/dealloying of the lithium to the lead. This reaction can be described in the following equation (2):

$$PbO_2 + xLi+ + xe^- \rightarrow Pb + Li_2O \ldots (2)$$

Since the lead carbon fibers also contain fibers, the lithium ions also intercalate with the carbon and equation (1) also applies in this electrochemical reaction since the lithium is reacting to both alloying/dealloying with the lead and intercalation/deintercalation with the carbon.

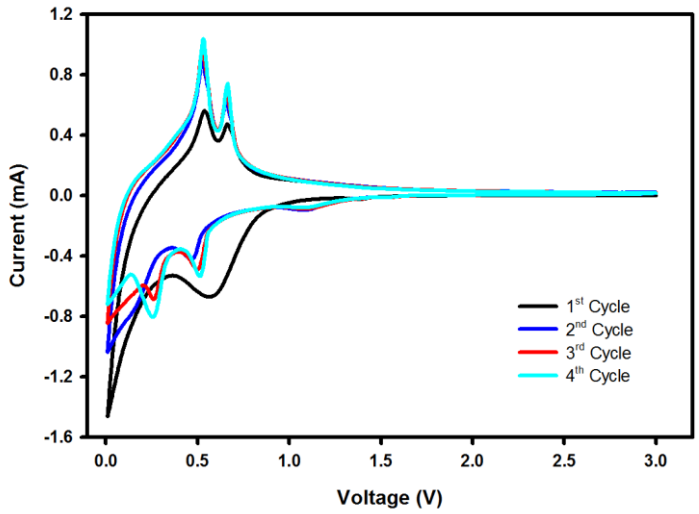

Figure 36 – Cyclic Voltammetry of lead carbon fibers between 0.01 and 3.0 V at a scan rate of 0.1 mVs^{-1}

5.2.3 Rate Performance

Rate performance tests were done to observe the performance of a lead carbon on a half-cell lithium ion battery. As shown in Figure 37, the rate performances of the anodes correlate with previous cycle performance tests. On the cyclic performance by the 100^{th} cycle the specific capacity of the lead carbon nanofibers was 270 $mAhg^{-1}$ and by the end of the rate performance test the specific capacity after being discharged through different current densities was 274 $mAhg^{-1}$.

The second set of cycling was done at 50 mAg^{-1} and it matches with the cycle performance tests done. The last cycle on the first set of 50 mAg^{-1} yielded 303 $mAhg^{-1}$ and the last set of 50 mAg^{-1} yielded an average of 276 $mAhg^{-1}$ Once the battery was finished discharging at 500 mAg^{-1}, it was discharged at 50 mAg^{-1} for the last 10 cycles and it stabilized at the approximately the same specific capacity on which the first set finished. This shows how stable

the lead carbon anode fibers are. The anode did not lost capacitance at any point even when the current density increased.

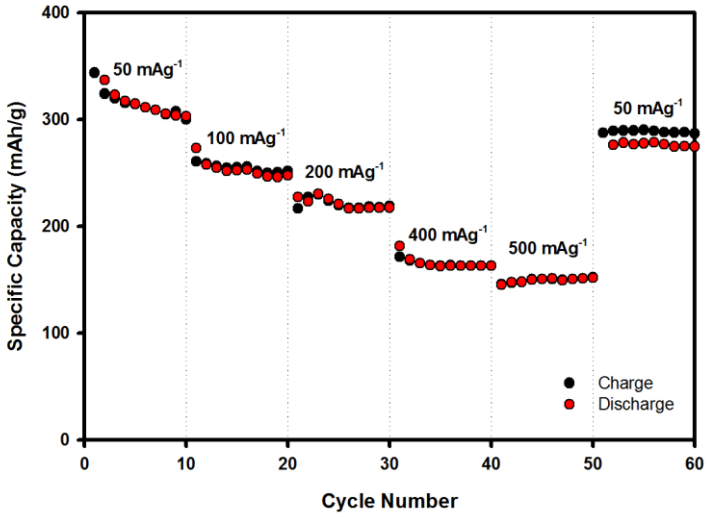

Figure 37 – Rate performance for the lead carbon anode performed at current densities of 50, 100, 200, 400 and 500 mAg^{-1}.

Another observation on the rate performance is how well the specific capacity of the lead carbon anode retained even when the current density is increased. When the current density increased to 100, 200, 400, and 500 $mAhg^{-1}$, the lead carbon anode retained 90.1, 91.9, 83.4 and 88.9% of its specific capacity from the previous current density it was cycling.

5.3 Post Mortem Analysis

A post mortem analysis was conducted to one of the half-cell lithium-ion batteries. Even though none of the batteries failed, it is important to see what changes happened to the anode after it cycled 100 times.

5.3.1 SEM

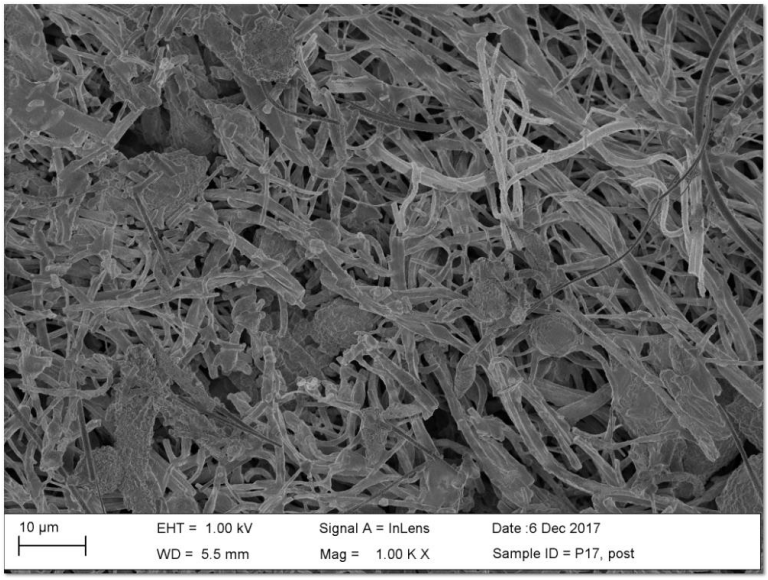

Figure 38 – SEM imaging of the post cycled lead carbon anode at 1KX.

Figure 38 it shows that the fibers seemed to be covered uniformly across the surface. This is more apparent as the magnification is increased on the SEM as shown in Figures 39, 40 and 41. One of the major concerns of using Pb on Li as mentioned in the literature review was the alloying/dealloying process that would increase the volume of the electrode and potentially would cause cracking and ultimately loss of specific capacity.

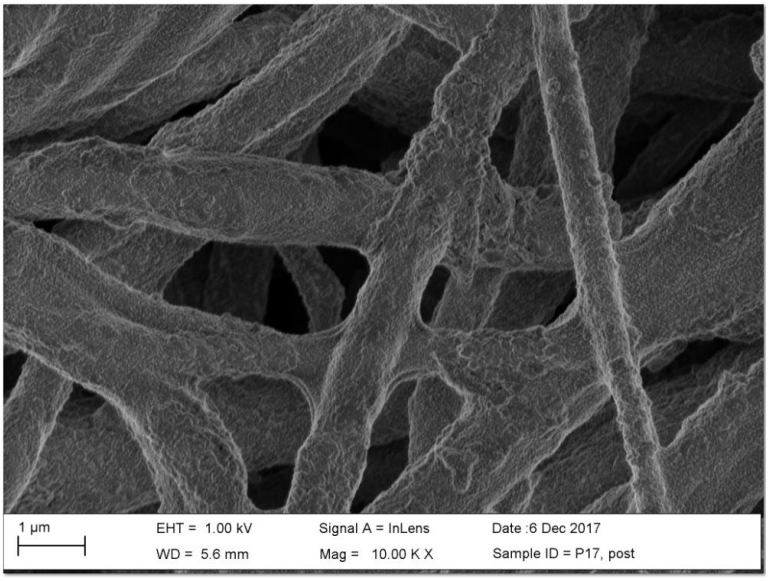

Figure 39 - SEM imaging of the post cycled lead carbon anode at 10KX.

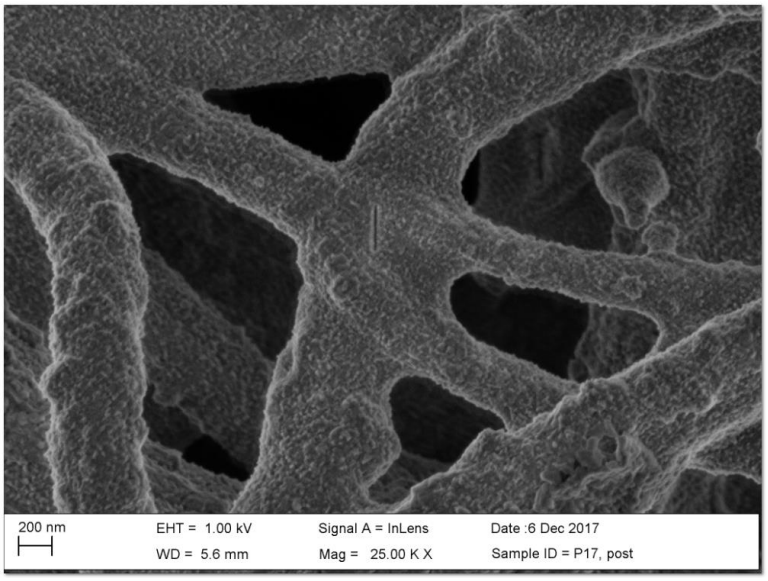

Figure 40 - SEM imaging of the post cycled lead carbon anode at 25KX.

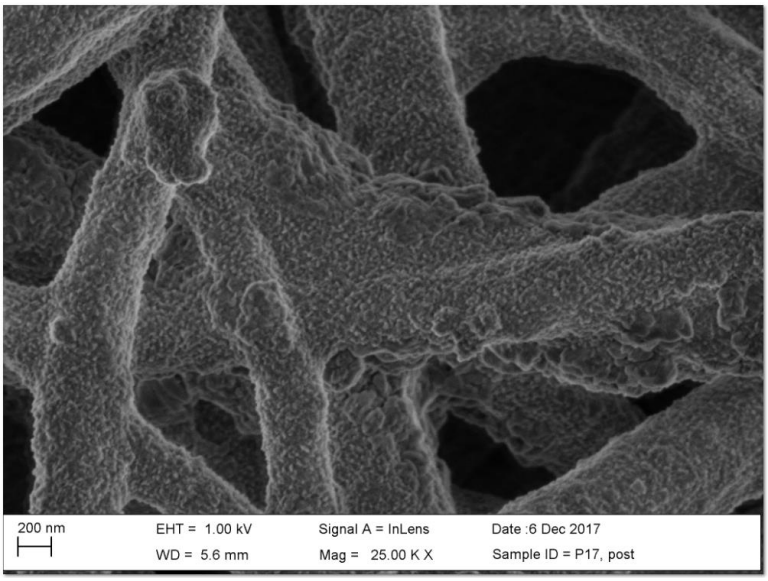

Figure 41 - SEM imaging of the post cycled lead carbon anode at 25KX.

When inspecting the SEM images there is not any evidence of the fibers becoming fractured. This can be credited to the carbon within the nanofibers that helped being the buffer for the volume change. As shown earlier in the electrochemical tests, the lead carbon nanofiber anode performed very stable throughout 100 cycles and could have potentially continued cycled more.

5.3.2 EDS

It is evident through the EDS mapping that the surface is covered by the electrolyte residue and that the anode has oxidized compared to how it was prior the electrochemical tests.

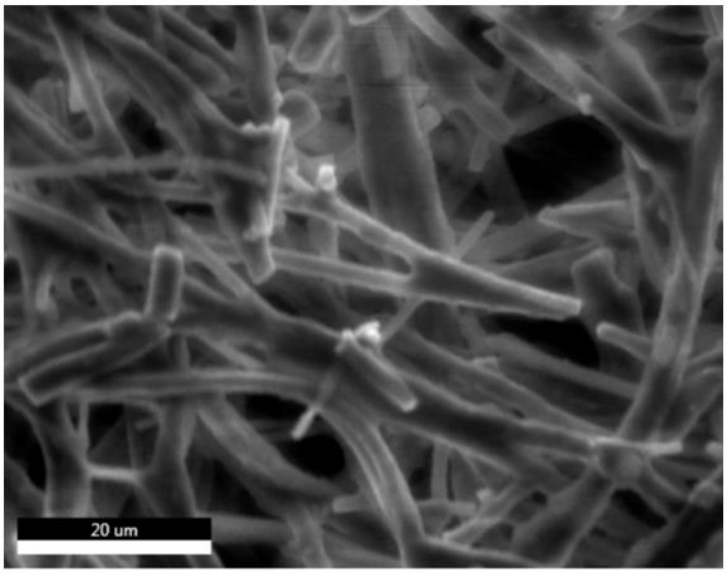

Figure 42 – EDS image for the post cycled lead carbon anode.

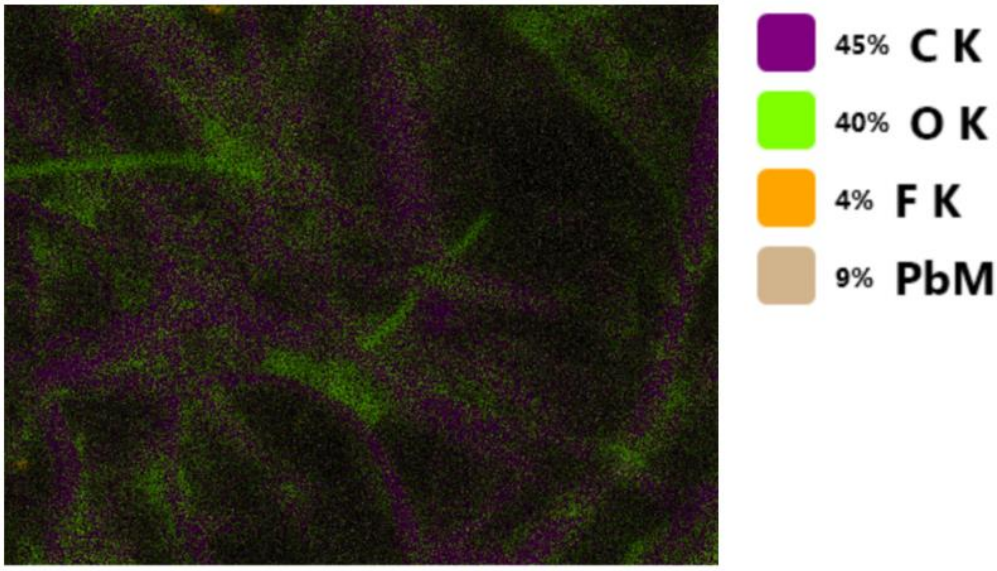

Figure 43 – Elemental analysis mapping for the post cycled lead carbon anode.

5.4 Discussion

Battery performance for the lead carbon anode showed to be stable and reliable for 100 cycles at difference discharge densities as shown in Fig 44. This is promising given that it shows the reliability of this anode and its ability to retain its specific capacity through various cycles.

Some of the major drawbacks of this research was the production of making the fibers "battery-ready," which is to be producing fibers that are lead-doped carbon and still flexible. When using the procedures done on previous experimentation the fibers would either come out losing the lead material or simply be too fragile to even handle without it completely disintegrating.

The process that ended up helping the fibers from retaining lead and retain some of its flexibility was to pre-expose the fibers to a lower heat that the carbonization process would force it to while the temperature is ramping up. By oxidizing the mat for approximately 24 hours at 120°C helped retain some to all the flexibility properties that the fibers had prior carbonization and made these fibers good for battery testing.

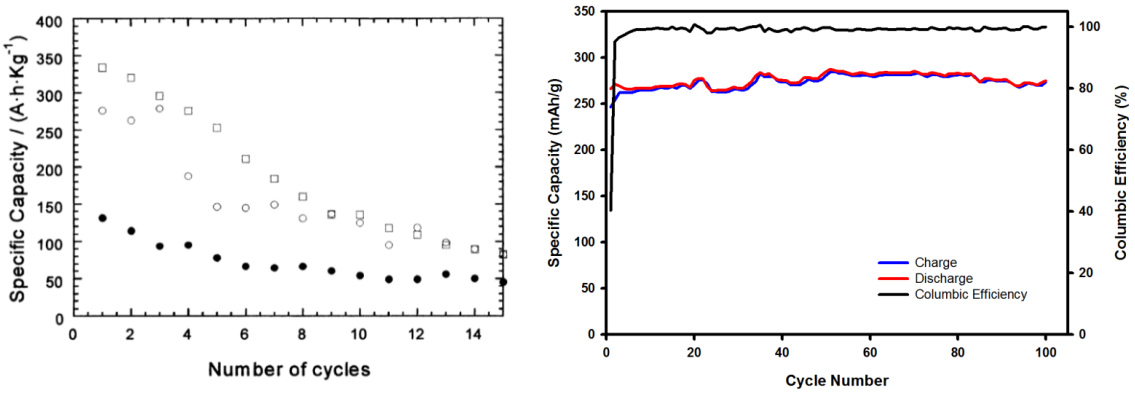

Figure 44 – Comparison from the specific capacities from the study mentioned earlier compared to results gathered in the lab with the lead carbon anode.[21]

When comparing the results gathered to what previous results have shown there has been major improvements to the performance of the battery. The specific capacity of the lead-carbon anode performed very stable and did not lose any significant capacitance throughout the 100 cycles it was tested. However, when three different materials were used in the study in 2002, all three decreased in the specific capacity significantly by the 15^{th} cycle whereas in the current lead carbon anode it did not.[21] By the 15^{th} cycle, the specific capacity of the lead carbon anode was 255 mAh/g^{-1} compared to the approx. 45 and 85 mAh/g^{-1}, which yields to an improvement of 467% and 200%, respectively.

CHAPTER VI

CONCLUSION & FUTURE WORK

6.1 Conclusion

Lead-doped carbon nanofibers were developed from Polyvinyl Alcohol (PVA) with Lead (II) Acetate by using the Forcespinning® technology. These fibers were stabilized for 25 hours at 125°C prior carbonizing them at 850°C in an Argon atmosphere. The lead carbon nanofibers diameter ranged from 250 - 750 nm and the lead contained in these fibers were found to be as high as 44% concentration after calcination at 850°C.

This is the first reported time of lead carbon fibers have been produced and tested for battery applications. Electrochemical tests were performed on half coin cell LIB with lead carbon nanofibers being used as the anode. Tests showed improved results to what previous studies have reported, having improvements of 200% to 467%, respectively. By creating a lead carbon anode, it showed 51% improvement with a stable specific capacity of 270 $mAhg^{-1}$ under the same parameters compared to the carbon anode. Cyclic Voltammetry showed that the anode undergoes an alloying/dealloying reaction with lithium during the electrochemical reaction within the cell and rate performance showed that the nanofibers stable cycling capacity. The lead carbon anode shows promise that it can be used as electrode replacements for future batteries for either LAB and/or LIB applications. These fibers demonstrated great cycling stability, stable specific capacity and capacity retention at 100 cycles.

Post mortem analysis showed the fibers still integral and potentially could have lasted more cycles before the battery failed. This can be attributed to the carbon within the lead fibers to have acted as a buffer from breaking down the fiber and causing the anode to lose capacitance and eventually leading the battery to fail.

6.2 Future Work

Future work could be to explore the possibility of increasing the quantity of lead contained in the fibers by using the forcespinning technology given that it is an inexpensive way to yield high quantities of nanofibers compared to its counterparts (electrospinning, electrospinning-centrifugal spinning, etc.).

On LABs, testing the lead nanofibers as potential negative added material or positive added material in an all lead-acid battery environment should be investigated to compare its performance to other lead-acid battery types. This could reduce the size and weight of LAB used in the SLI market which could bring manufacturers and consumers savings over time.

On LIBs, by having more stable materials and reduce the possibility of violent reactions should be investigated. In all electrochemical tests, the batteries were still operational at the end of 100 cycles. The specific capacity of the lead-carbon anode did not fluctuate, additional tests could also be done to see how many cycles that battery can perform until failure.

REFERENCES

(1) Kurzweil, P. Gaston Plant?? And His Invention of the Lead-Acid Battery-The Genesis of the First Practical Rechargeable Battery. *J. Power Sources* **2010**, *195*, 4424–4434.

(2) Krieger, E. M.; Cannarella, J.; Arnold, C. B. A Comparison of Lead-Acid and Lithium-Based Battery Behavior and Capacity Fade in off-Grid Renewable Charging Applications. *Energy* **2013**, *60*, 492–500.

(3) Kovala, T.; Matikainen, E.; Mannelin, T.; Erkkilä, J.; Riihimäki, V.; Hänninen, H.; Aitio, a. Effects of Low Level Exposure to Lead on Neurophysiological Functions among Lead Battery Workers. *Occup. Environ. Med.* **1997**, *54*, 487–493.

(4) Garche, J.; Moseley, P. T.; Karden, E. *Lead–acid Batteries for Hybrid Electric Vehicles and Battery Electric Vehicles*; Elsevier Ltd., 2015.

(5) Enos, D. G. *Lead-Acid Batteries for Medium- and Large-Scale Energy Storage*; Elsevier Ltd., 2015.

(6) Nuzhny, A. Corrosion of Low-Antimony Lead-Cadmium Alloys in Conditions of Long-Term Polarization. *J. Power Sources* **2006**, *158*, 920–926.

(7) Rahmanifar, M. S. Enhancing the Cycle Life of Lead-Acid Batteries by Modifying Negative Grid Surface. *Electrochim. Acta* **2017**, *235*, 10–18.

(8) Hong, B.; Jiang, L.; Hao, K.; Liu, F.; Yu, X.; Xue, H.; Li, J.; Liu, Y. Al/Pb Lightweight Grids Prepared by Molten Salt Electroless Plating for Application in Lead-Acid Batteries. *J. Power Sources* **2014**, *256*, 294–300.

(9) Treptow, R. S. The Lead-Acid Battery: Its Voltage in Theory and in Practice. *J. Chem. Educ.* **2002**, *79*, 334.

(10) Student, M. I. T. II . Equilibrium Thermodynamics Lecture 9 : Fuel Cells and Lead-Acid Batteries. **2009**, 1–8.

(11) Moseley, P. T.; Rand, D. a J.; Monahov, B. Designing Lead-Acid Batteries to Meet Energy and Power Requirements of Future Automobiles. *J. Power Sources* **2012**, *219*, 75–79.

(12) Gore, I. G. E.; Branch, N.; Roman, T.; Orange, E.; Wayne, K.; Gore, R. A. United States Patent (19). **1998**.

(13) Catherino, H. a.; Feres, F. F.; Trinidad, F. Sulfation in Lead-Acid Batteries. *J. Power Sources* **2004**, *129*, 113–120.

(14) Ruetschi, P. Aging Mechanisms and Service Life of Lead-Acid Batteries. *J. Power Sources* **2004**, *127*, 33–44.

(15) Lithium Energy Diagram, https://www.cei.washington.edu/wordpress/wp-content/uploads/2015/11/li-energy-density.gif .

(16) De Las Casas, C.; Li, W. A Review of Application of Carbon Nanotubes for Lithium Ion Battery Anode Material. *J. Power Sources* **2012**, *208*, 74–85.

(17) Zhou, H.; Ding, X.; Liu, G.; Jiang, Y.; Yin, Z.; Wang, X. Preparation and Characterization of Ultralong Spinel Lithium Manganese Oxide Nanofiber Cathode via Electrospinning Method. *Electrochim. Acta* **2015**, *152*, 274–279.

(18) Yang, G.; Wang, L.; Wang, J.; Wei, W.; Yan, W. Fabrication of Lithium Manganese Oxide Nanoribbons by Electrospinning: A General Strategy and Formation Mechanism. *Mater. Des.* **2016**, *112*, 429–435.

(19) Sin, D. Y.; Koo, B. R.; Ahn, H. J. Hollow Lithium Manganese Oxide Nanotubes Using MnO2-Carbon Nanofiber Composites as Cathode Materials for Hybrid Capacitors. *J. Alloys Compd.* **2017**, *696*, 290–294.

(20) Ji, L.; Lin, Z.; Alcoutlabi, M.; Zhang, X. Recent Developments in Nanostructured Anode Materials for Rechargeable Lithium-Ion Batteries. *Energy Environ. Sci.* **2011**, *4*, 2682.

(21) Martos, M.; Morales, J.; Sánchez, L. Lead-Based Systems as Suitable Anode Materials for Li-Ion Batteries. *Electrochim. Acta* **2003**, *48*, 615–621.

(22) Park, C.-M.; Kim, J.-H.; Kim, H.; Sohn, H.-J. Li-Alloy Based Anode Materials for Li Secondary Batteries. *Chem. Soc. Rev.* **2010**, *39*, 3115.

(23) Zhang, J.-G.; Xu, W.; Henderson, W. A. *Lithium Metal Anodes and Rechargeable Lithium Metal Batteries*; 2017; Vol. 249.

(24) Catherino, H. a. Complexity in Battery Systems: Thermal Runaway in VRLA Batteries. *J. Power Sources* **2006**, *158*, 977–986.

(25) Hall, H.; Fasih, A. Modeling and Fault Diagnosis of Automotive Lead-Acid Batteries Dr Giorgio Rizzoni , Advisor. **2006**.

(26) Suresh, R.; Rengaswamy, R. *Capacity Fade Minimizing Model Predictive Control Approach for the Identification and Realization of Charge-Discharge Cycles in Lithium Ion Batteries*; Elsevier Masson SAS, 2017; Vol. 40.

(27) Mccormac, K. Electrospun Titanium Dioxide and Silicon Composite Nanofibers for Advanced Lithium Ion Batteries Electrospun Titanium Dioxide and Silicon Composite Nanofibers for Advanced Lithium Ion Batteries. **2015**, 1–5.

(28) Bača, P.; Micka, K.; Křivík, P.; Tonar, K.; Tošer, P. Study of the Influence of Carbon on the Negative Lead-Acid Battery Electrodes. *J. Power Sources* **2011**, *196*, 3988–3992.

(29) Xiang, J.; Ding, P.; Zhang, H.; Wu, X.; Chen, J.; Yang, Y. Beneficial Effects of Activated

Carbon Additives on the Performance of Negative Lead-Acid Battery Electrode for High-Rate Partial-State-of-Charge Operation. *J. Power Sources* **2013**, *241*, 150–158.

(30) Pavlov, D.; Nikolov, P.; Rogachev, T. Influence of Carbons on the Structure of the Negative Active Material of Lead-Acid Batteries and on Battery Performance. *J. Power Sources* **2011**, *196*, 5155–5167.

(31) Boden, D. P.; Loosemore, D. V.; Spence, M. a.; Wojcinski, T. D. Optimization Studies of Carbon Additives to Negative Active Material for the Purpose of Extending the Life of VRLA Batteries in High-Rate Partial-State-of-Charge Operation. *J. Power Sources* **2010**, *195*, 4470–4493.

(32) Kirchev, A.; Kircheva, N.; Perrin, M. Carbon Honeycomb Grids for Advanced Lead-Acid Batteries. Part I: Proof of Concept. *J. Power Sources* **2011**, *196*, 8773–8788.

(33) Hong, B.; Jiang, L.; Xue, H.; Liu, F.; Jia, M.; Li, J.; Liu, Y. Characterization of Nano-Lead-Doped Active Carbon and Its Application in Lead-Acid Battery. *J. Power Sources* **2014**, *270*, 332–341.

(34) Moseley, P. T.; Nelson, R. F.; Hollenkamp, a. F. The Role of Carbon in Valve-Regulated Lead-Acid Battery Technology. *J. Power Sources* **2006**, *157*, 3–10.

(35) Kozawa, A.; Oho, H.; Sano, M.; Brodd, D.; Brodd, R. Beneficial Effect of Carbon – PVA Colloid Additives for Lead – Acid Batteries. **1999**, 12–16.

(36) Wang, H.; Yu, J.; Zhao, Y.; Guo, Q. A Facile Route for PbO@C Nanocomposites: An Electrode Candidate for Lead-Acid Batteries with Enhanced Capacitance. *J. Power Sources* **2013**, *224*, 125–131.

(37) Moseley, P. T.; Rand, D. a. J.; Peters, K. Enhancing the Performance of Lead–acid Batteries with Carbon – In Pursuit of an Understanding. *J. Power Sources* **2015**, *295*, 268–274.

(38) Zhang, Y.; Jiao, Y.; Liao, M.; Wang, B.; Peng, H. Carbon Nanomaterials for Flexible Lithium Ion Batteries. *Carbon N. Y.* **2017**, *124*, 79–88.

(39) Wang, C.; Chen, B.; Yu, Y.; Wang, Y.; Zhang, W. Carbon Footprint Analysis of Lithium Ion Secondary Battery Industry: Two Case Studies from China. *J. Clean. Prod.* **2017**, *163*, 241–251.

(40) Jaiswal, A.; Chalasani, S. C. The Role of Carbon in the Negative Plate of the Lead–acid Battery. *J. Energy Storage* **2015**, *1*, 15–21.

(41) Ji, L.; Zhang, X. Generation of Activated Carbon Nanofibers from Electrospun Polyacrylonitrile-Zinc Chloride Composites for Use as Anodes in Lithium-Ion Batteries. *Electrochem. commun.* **2009**, *11*, 684–687.

(42) Xiang, J.; Lv, W.; Mu, C.; Zhao, J.; Wang, B. Activated Hard Carbon from Orange Peel for Lithium/Sodium Ion Battery Anode with Long Cycle Life. *J. Alloys Compd.* **2017**, *701*, 870–874.

(43) Zaghib, K.; Striebel, K.; Guerfi, a.; Shim, J.; Armand, M.; Gauthier, M. LiFePO4/Polymer/Natural Graphite: Low Cost Li-Ion Batteries. *Electrochim. Acta* **2004**, *50*, 263–270.

(44) Fernández, M.; Valenciano, J.; Trinidad, F.; Muñoz, N. The Use of Activated Carbon and Graphite for the Development of Lead-Acid Batteries for Hybrid Vehicle Applications. *J. Power Sources* **2010**, *195*, 4458–4469.

(45) Wonsawat, W.; Chuanuwatanakul, S.; Dungchai, W.; Punrat, E.; Motomizu, S.; Chailapakul, O. Graphene-Carbon Paste Electrode for Cadmium and Lead Ion Monitoring in a Flow-Based System. *Talanta* **2012**, *100*, 282–289.

(46) Cremar, L. D.; Acosta-martinez, J.; Villarreal, A.; Salinas, A.; Mao, Y.; Lozano, K. Multifunctional Carbon Nanofiber Systems Mass Produced from Water Soluble Polymers and Low Temperature Processes. *Text. Technol. - Chem. Fibers Int. Fiber Prod. No 1, Doc. 6* **2016**, 1–17.

(47) Cremar, L. D.; Acosta-Martinez, J.; Villarreal, A.; Salinas, A.; Lozano, K. Mechanical and Electrical Characterization of Carbon Nanofibers Produced from Water Soluble Precursors. *Mater. Today Commun.* **2016**, *7*, 134–139.

(48) Swogger, S. W.; Everill, P.; Dubey, D. P.; Sugumaran, N. Discrete Carbon Nanotubes Increase Lead Acid Battery Charge Acceptance and Performance. *J. Power Sources* **2014**, *261*, 55–63.

(49) Sugumaran, N.; Everill, P.; Swogger, S. W.; Dubey, D. P. Lead Acid Battery Performance and Cycle Life Increased through Addition of Discrete Carbon Nanotubes to Both Electrodes. *J. Power Sources* **2015**, *279*, 281–293.

(50) Marom, R.; Ziv, B.; Banerjee, A.; Cahana, B.; Luski, S.; Aurbach, D. Enhanced Performance of Starter Lighting Ignition Type Lead-Acid Batteries with Carbon Nanotubes as an Additive to the Active Mass. *J. Power Sources* **2015**, *296*, 78–85.

(51) Sehrawat, P.; Julien, C.; Islam, S. S. Carbon Nanotubes in Li-Ion Batteries: A Review. *Mater. Sci. Eng. B Solid-State Mater. Adv. Technol.* **2016**, *213*, 12–40.

(52) Jestin, S.; Poulin, P. *Wet Spinning of CNT-Based Fibers*; Elsevier, 2013.

(53) Ozipek, B.; Karakas, H. *Wet Spinning of Synthetic Polymer Fibers.*; Woodhead Publishing Limited, 2014; Vol. 150.

(54) Imura, B (New Jersey Institute of Technology, U.; Hogan, H (Omni Tech International, U.; Jaffe, M(New Jersey Instittute of Technology, U. *Dry Spinning of Synthetic Polymer Fibers*; Woodhead Publishing Limited, 2014.

(55) Kutlu, B.; Meinl, J.; Leuteritz, A.; Brünig, H.; Heinrich, G. Melt-Spinning of LDH/HDPE Nanocomposites. *Polym. (United Kingdom)* **2013**, *54*, 5712–5718.

(56) Chronakis, I. S. *Micro- and Nano-Fibers by Electrospinning Technology*; Second Edi.; Yi Qin, 2015.

(57) Doshi, J.; Reneker, D. H. Electrospinning Process and Applications of Electrospun Fibers. *Conf. Rec. 1993 IEEE Ind. Appl. Conf. Twenty-Eighth IAS Annu. Meet.* **1993**, *35*, 151–160.

(58) Li, D.; Xia, Y. Electrospinning of Nanofibers: Reinventing the Wheel? *Adv. Mater.* **2004**, *16*, 1151–1170.

(59) Rutledge, G. C.; Fridrikh, S. V. Formation of Fibers by Electrospinning. *Adv. Drug Deliv. Rev.* **2007**, *59*, 1384–1391.

(60) Greiner, A.; Wendorff, J. H. Electrospinning: A Fascinating Method for the Preparation of Ultrathin Fibers. *Angew. Chemie - Int. Ed.* **2007**, *46*, 5670–5703.

(61) Dharmaraj, N.; Kim, C. H.; Kim, H. Y. Pb(Zr0.5, Ti0.5)O3 Nanofibres by Electrospinning. *Mater. Lett.* **2005**, *59*, 3085–3089.

(62) Santiago-Aviles, J. J.; Wang, Y.; Furlan, R.; Ramos, I. Synthesis and Characterization of Micro/Nanoscopic Pb(Zr 0.52 Ti 0.48)O 3 Fibers by Electrospinning. *Appl. Phys. A Mater. Sci. Process.* **2004**, *78*, 1043–1047.

(63) Sarkar, K.; Gomez, C.; Zambrano, S.; Ramirez, M.; De Hoyos, E.; Vasquez, H.; Lozano, K. Electrospinning to Forcespinning™. *Mater. Today* **2010**, *13*, 12–14.

(64) Agubra, V. A.; Garza, D. De; Gallegos, L.; Alcoutlabi, M. ForceSpining V of Polyacrylonitrile for Mass Production of Lithium-Ion Battery Separators. **2015**, *00000*, 1–9.

(65) Pereira-da-silva, M. D. A.; Ferri, F. A. *1 - Scanning Electron Microscopy*; Elsevier Inc., 2017.

(66) Paredes, A. M. *MICROSCOPY | Scanning Electron Microscopy*; Second Edi.; Elsevier, 2014; Vol. 2.

(67) Henning, S.; Adhikari, R. *Chapter 1 - Scanning Electron Microscopy, ESEM, and X-Ray Microanalysis A2 - Thomas, Sabu*; Elsevier Inc., 2017.

(68) Abd Mutalib, M.; Rahman, M. A.; Othman, M. H. D.; Ismail, A. F.; Jaafar, J. *Scanning Electron Microscopy (SEM) and Energy-Dispersive X-Ray (EDX) Spectroscopy*; Elsevier B.V., 2017.

(69) Wagner, M. Thermogravimetric Analysis. *Therm. Anal. Pract.* **2017**, 162–186.

(70) Sauerbrunn, S.; Gill, P. Decomposition Kinetics Using TGA. *TA Instruments TA-075*.

(71) Aziz, M.; Ismail, A. F. X-Ray Photoelectron Spectroscopy (XPS). *Membr. Charact.* **2017**, 81–93.

(72) Climent, V.; Feliu, J. M. *Cyclic Voltammetry*; Elsevier Inc., 2015.

(73) Cyclone, http://www.prweb.com/releases/nanofiber_production/equipment_award/prweb8622439.htm.

(74) Lu, X.; Zhao, Y.; Wang, C. Fabrication of PbS Nanoparticles in Polymer-Fiber Matrices by Electrospinning. *Adv. Mater.* **2005**, *17*, 2485–2488.

APPENDIX A

APPENDIX A

Table 1. State-of-the-Art Equipment

Equipment	Purpose	Results Obtained
Cyclone	Production of PVA and PVA-Pb nanofibers	Yielded PVA & PVA-Pb nanofibers.
Scanning Electron Microscope	To take images of the produced nanofibers	Captured images for PVA, PVA-Pb and lead carbon fibers. Results canbe found in Chapter 5.
Energy-dispersive X-Ray Spectroscopy	A qualitative method of determining the type of material the sample contains	Verified the materials that the fibers were composed off. Results can be found in Chapter 5.
Thermogravimetric Analysis	Thermal degradation of the PVA, PVA-Pb and lead carbon nanofibers	Obtained the temperatures where the fibers degraded. Results can be found in Chapter 5.
X-Ray Photoelectron Spectroscopy	A quantitative method of determining the type of material the sample contains	Verified the materials that the fibers were composed off. Results can be found in Chapter 5.
LANHE Battery Testing Systems	Performed Charge/Discharge on Li-ion Batteries	Successfully cycled batteries 100 times. Results can be found in Chapter 5.
Arbin Instruments	Performed Rate Performance on Lithium-ion Batteries	Successfully performed rate performance test. Results can be found in Chapter 5.
BioLogic Science Instruments	Performed Cyclic Voltammetry on Lithium-ion batteries	Successfully performed cyclic voltammetry tests. Results can be found in Chapter 5.

Table 2. State-of-the-Art Software

Software	Purpose	Results Obtained
Texture and Elemental Analytical Microscopy	Analysis of the Energy-dispersive X-ray Spectroscopy	Found material composition of the nanofibers. Results can be found in Chapter 5.
TA Analyzer	Analysis of TGA	Found deterioration points from samples. Results can be found in Chapter 5.
LAND Battery Testing System	Analysis of the Charge/Discharge tests	Verified that lead carbon nanofibers are a stable material to use as an anode. Results can be found in Chapter 5.
BT Lab	Analysis of the Cyclic Voltammetry	Acquired data to see chemical reactions that took place during charge and discharge. Results can be found in Chapter 5.
MITS Pro	Analysis of the Rate Performance	Verified that lead carbon nanofibers are a stable material to use as an anode. Results can be found in Chapter 5.
SigmaPlot	Software to plot data	Successfully plotted curves used in various figures in thesis.

BIOGRAPHICAL SKETCH

Omar Torres graduated on May 2011 with his Bachelors of Science in Mechanical Engineering at The University of Texas - Pan American. Prior graduation he completed 3-term co-op with Halliburton Energy Services where he began his Oil & Gas career in 2009. After working there for 2 semesters in 2009 and in 2010. He was hired for full-time as an Open-Hole Wireline Field Professional in 2011 until the end of the year in Kilgore, TX. He continued his career in the Oil & Gas profession from 2012 until the end of 2015 as a Logging-While-Drilling Field Professional working onshore and offshore in the Gulf of Mexico in various jackups and drillships.

In the summer of 2015, he was accepted to The University of Texas - Rio Grande Valley Graduate Program where he also began working as a Graduate Research Assistant for Dr. Karen Lozano in the Center for Nanotechnology. He defended and submitted his thesis in order to obtain his Master's degree on May 2018.

Email: omar.torres87@gmail.com
LinkedIn: www.linkedin.com/in/omartorres25